ZCO-68: Influence on fracture properties of galvanneal coating

J. Lian, J. He, N. Vajragupta, S. Münstermann, W. Bleck
Steel Institute, RWTH Aachen Univeristy, Germany

III

Accomplished results

Microstructure characterization
- Substrate characterization
- Coating characterization with TEM

Artificial microstructure model

Plasticity description of constituents
- Plasticity description of substrate
- Nanoindentation test on coating

Formability characterization
- Hole expansion test
- Nakajima test

Failure criterion identification
- In-situ bending test

Draft Final Report received May 5, 2017

Comparison of the stress-strain curve between GA DP980 (3 mm thickness) and EG DP980(1.5 mm thickness): (a) engineering stress-strain, (b) true stress-strain. Flow curves fitted using Swift equation

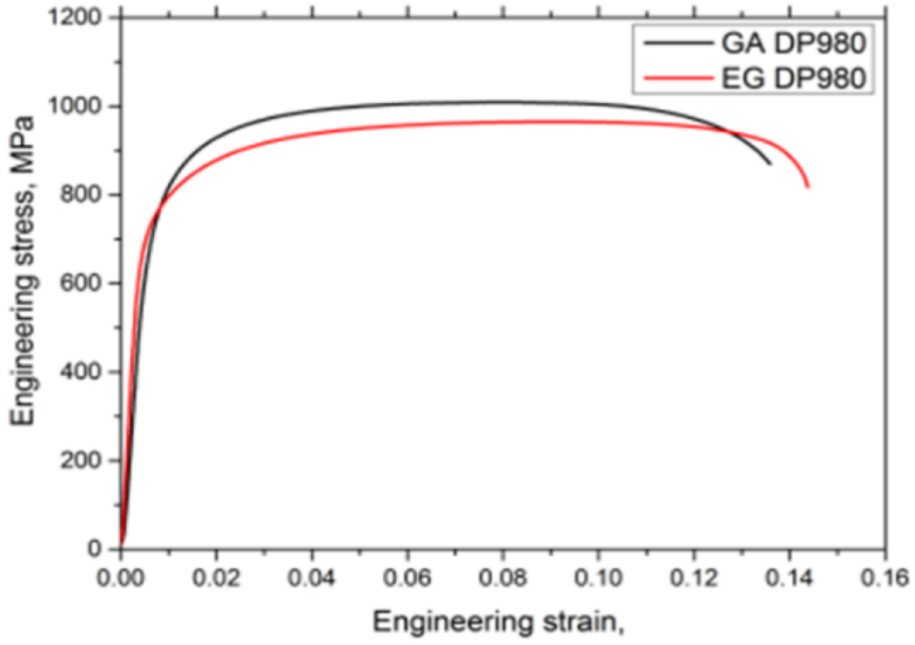

(a)

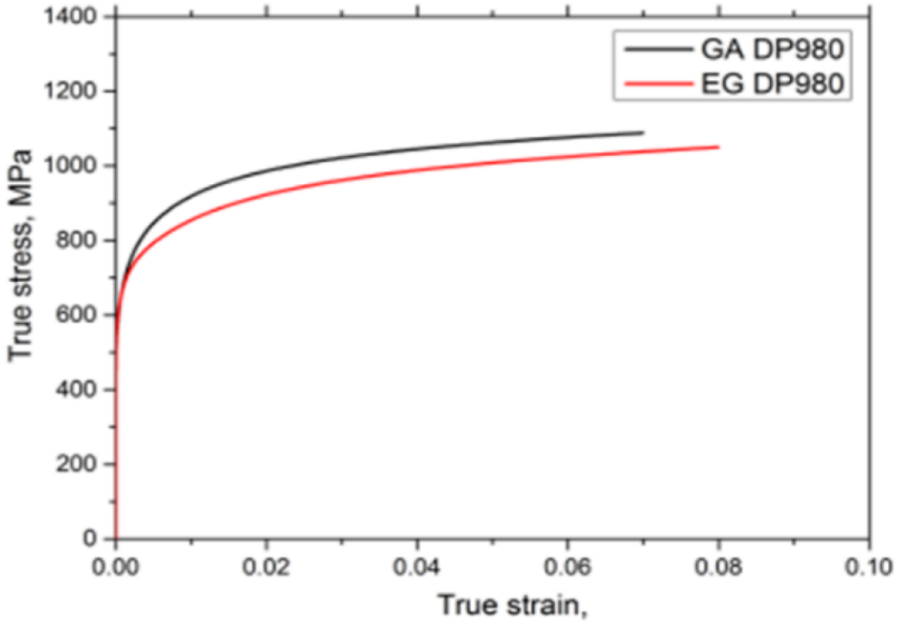

(b)

In-situ bending test in LC-SEM

Experimental setup

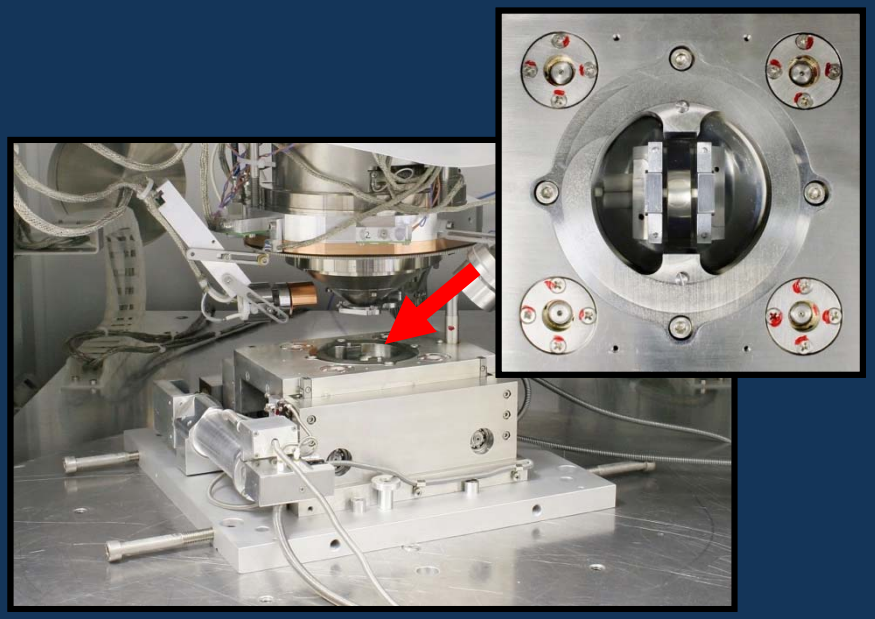

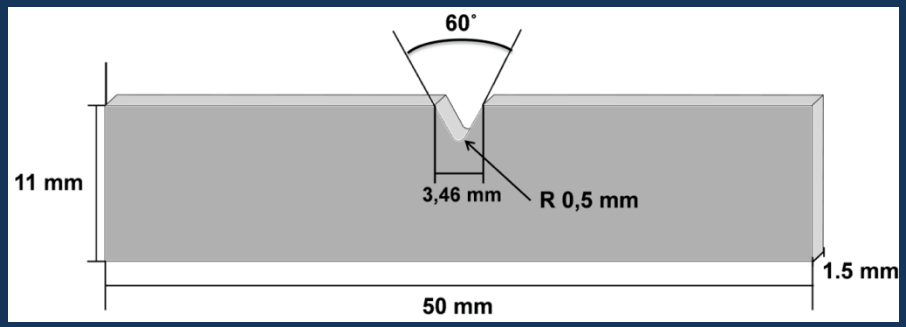

- The in-situ 3-point bending test is performed to characterize the failure behaviour.
- This identification is via SEM.
- Single-notched specimen is manufactured.

In-situ bending test in LC-SEM

Results: force-displacement response

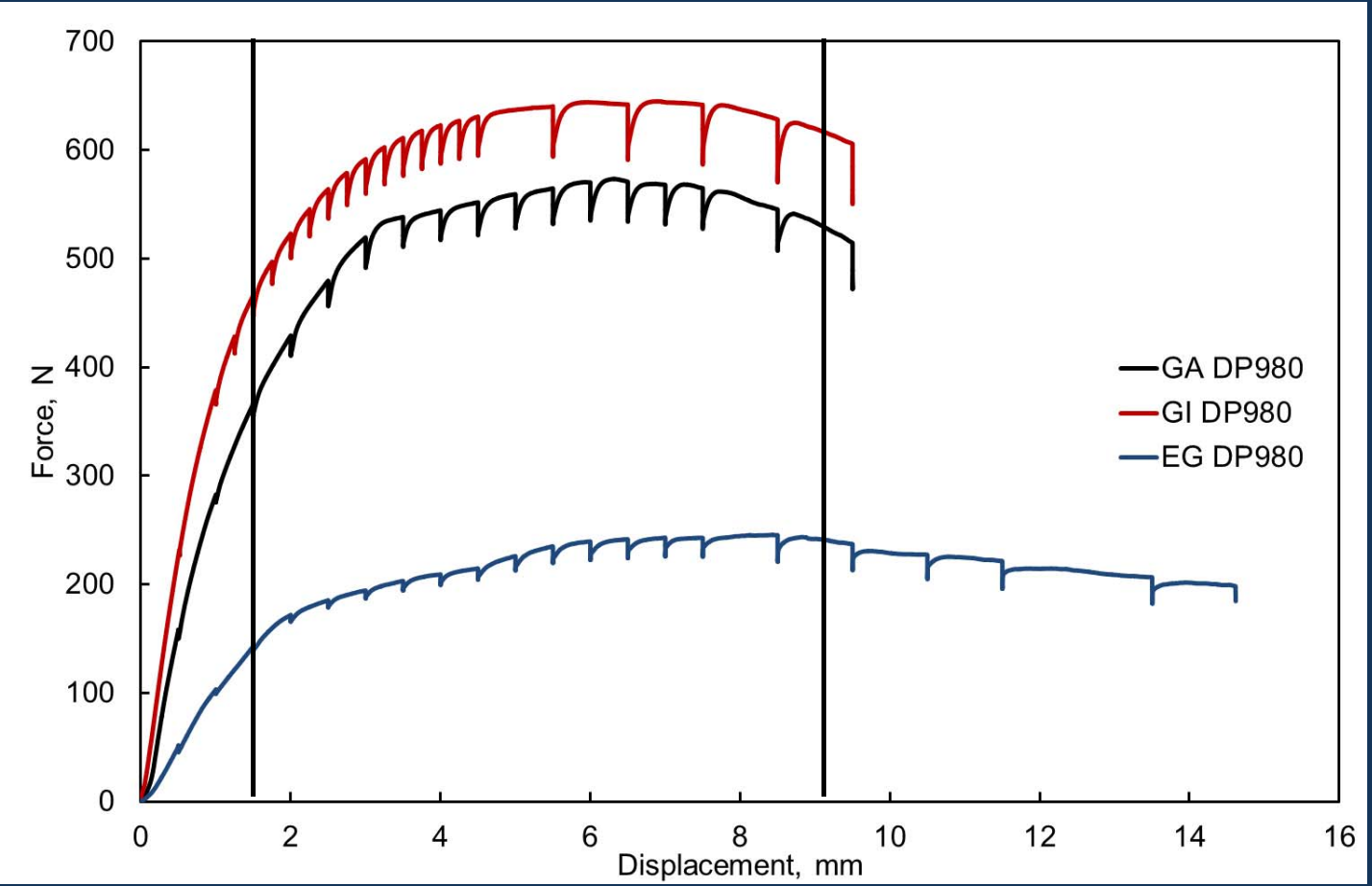

Note: GI and GA samples 3mm thick, EG 1.5 mm thick

Modified In-situ bending test in LC-SEM

Experimental setup

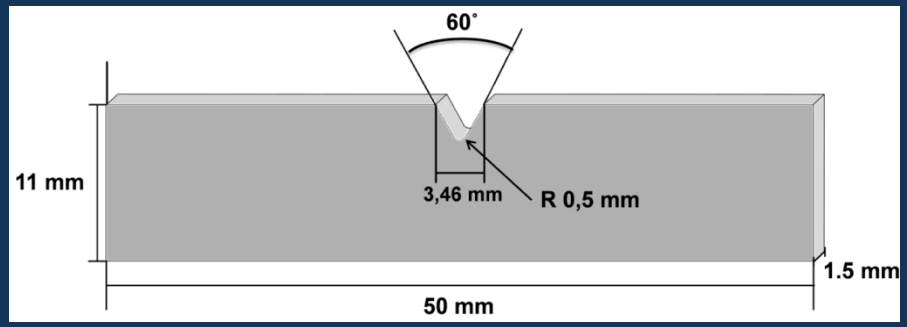

Regular in-situ bending test sample

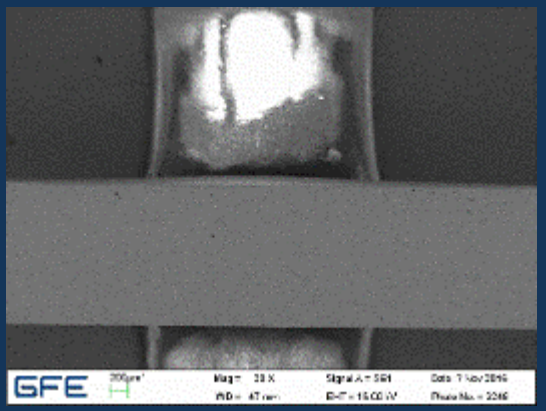

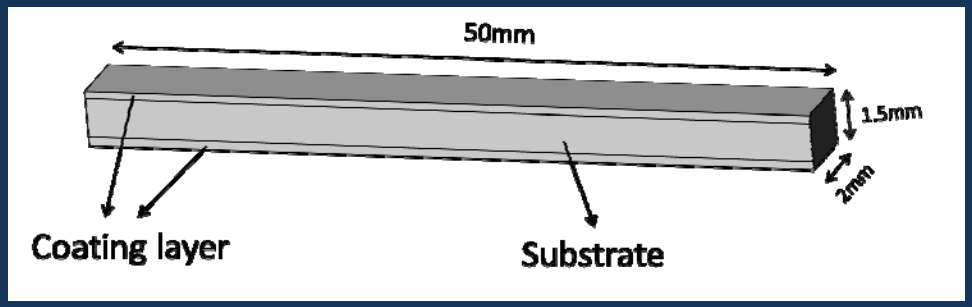

Modified in-situ bending test sample for coating layer fracture observation

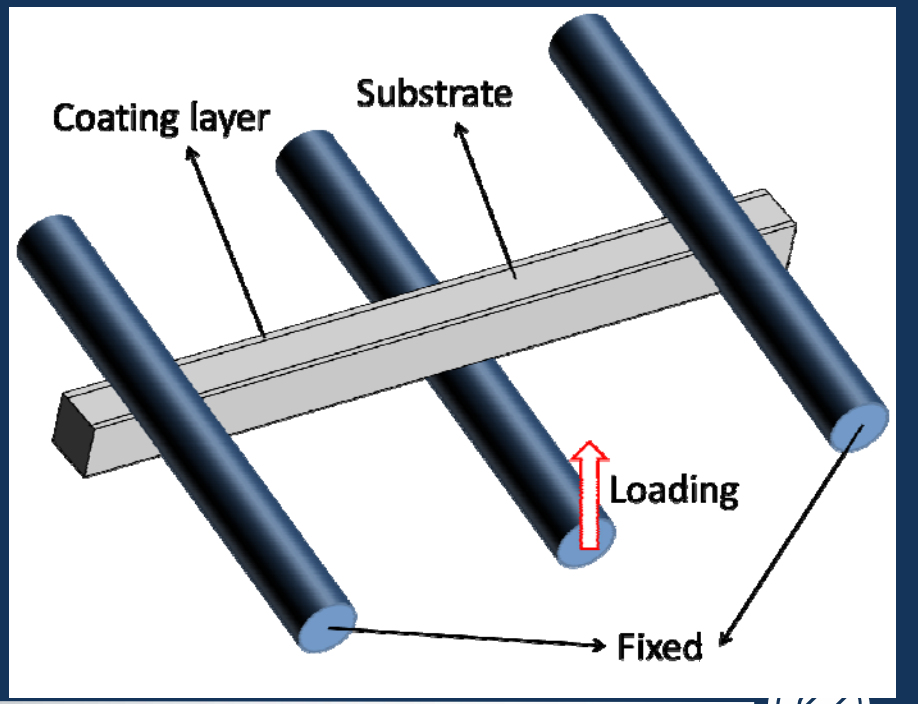

III

Formability and failure characterization

Modified In-situ bending test in LC-SEM

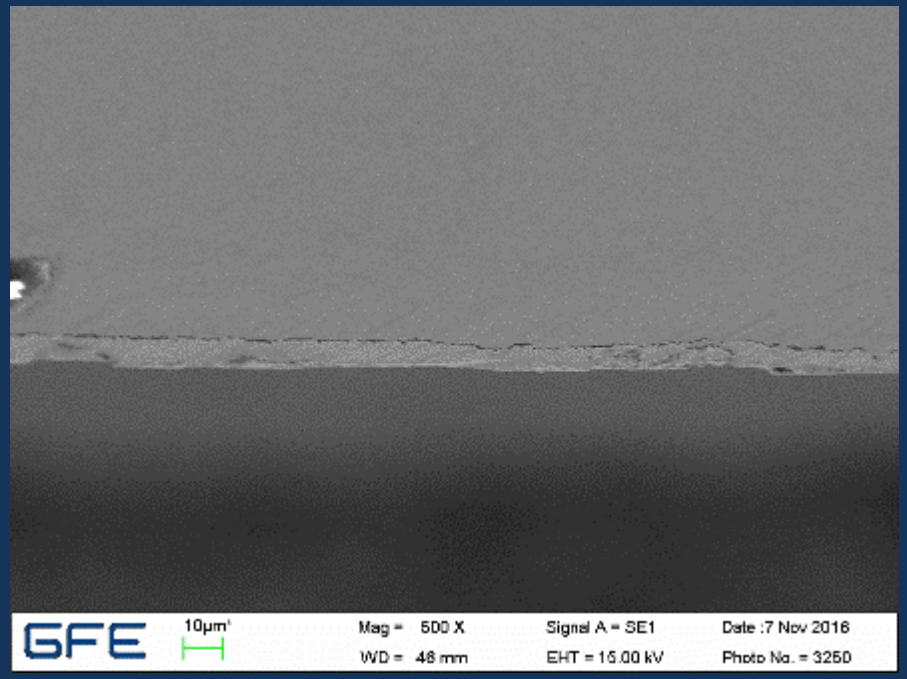

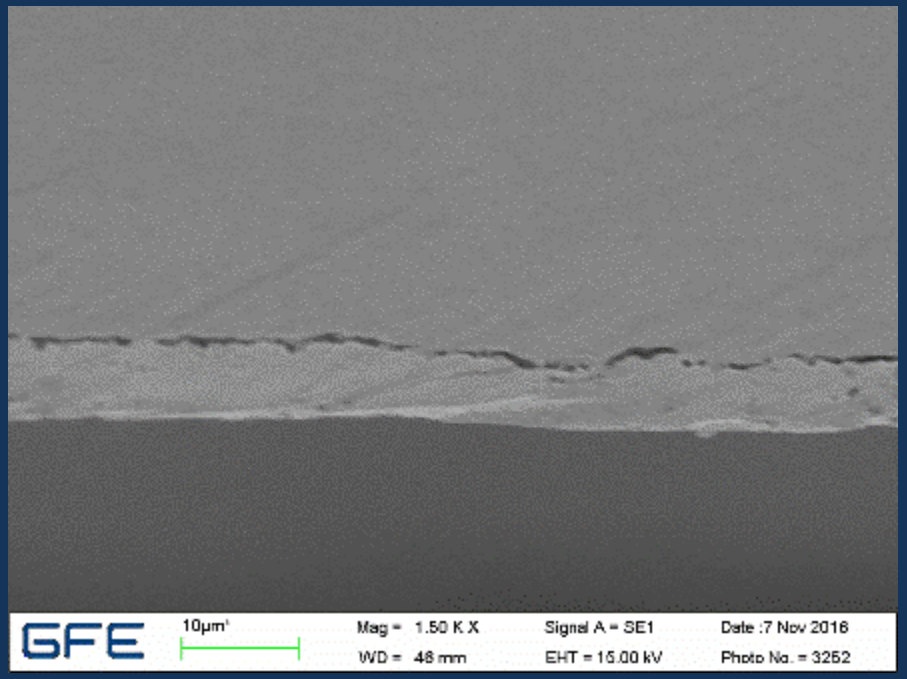

0 mm

0 mm

GA DP980

III

Formability and failure characterization

Modified In-situ bending test in LC-SEM

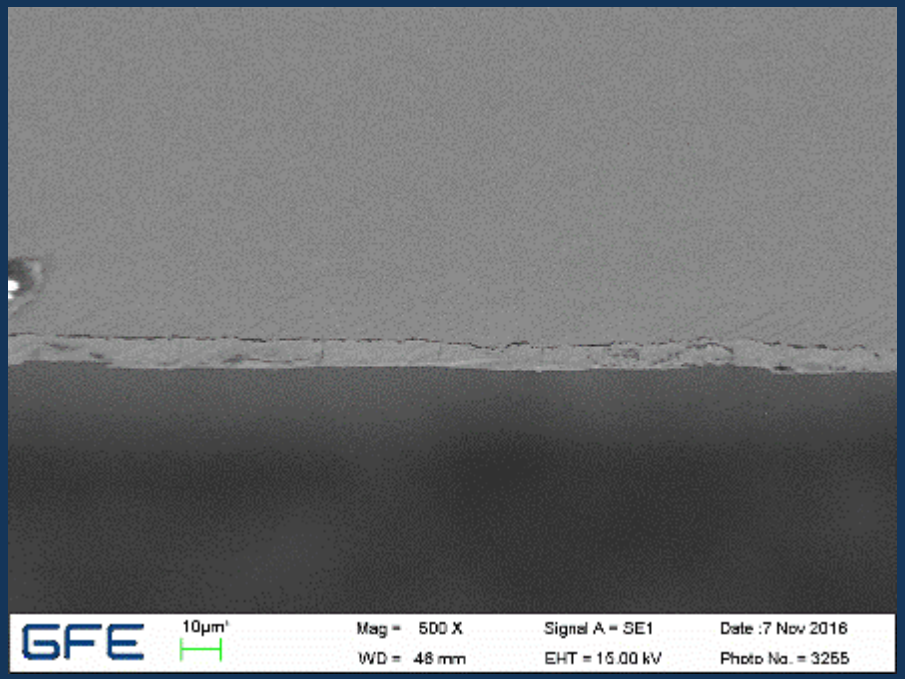

0.5 mm

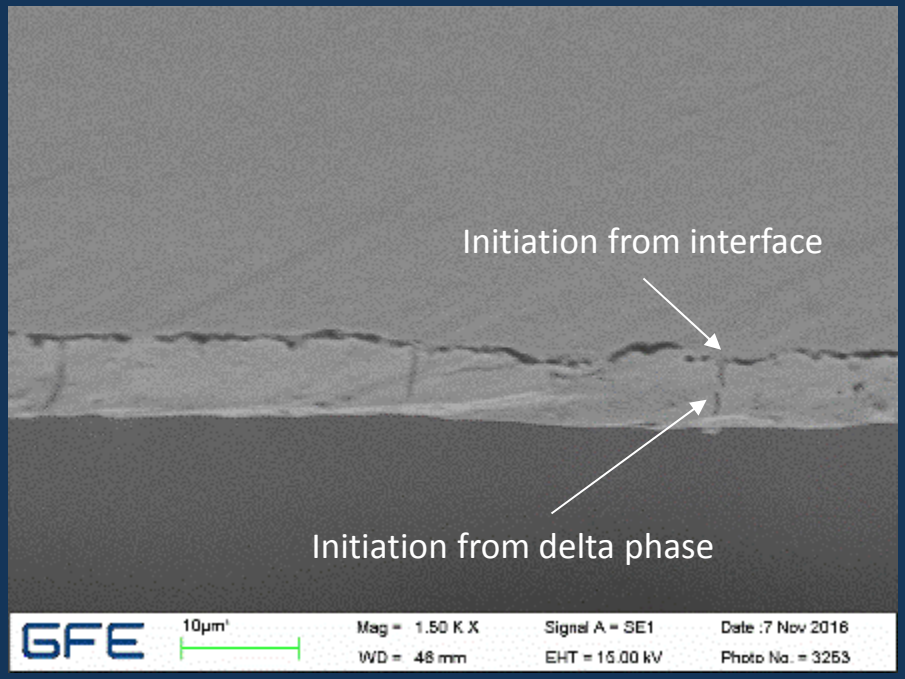

0.5 mm

GA DP980

Coating	Gamma, µm	Delta, µm	Zeta, µm	Eta, µm
GA	0.465	4.380	3.265	-

III

Formability and failure characterization

Modified In-situ bending test in LC-SEM

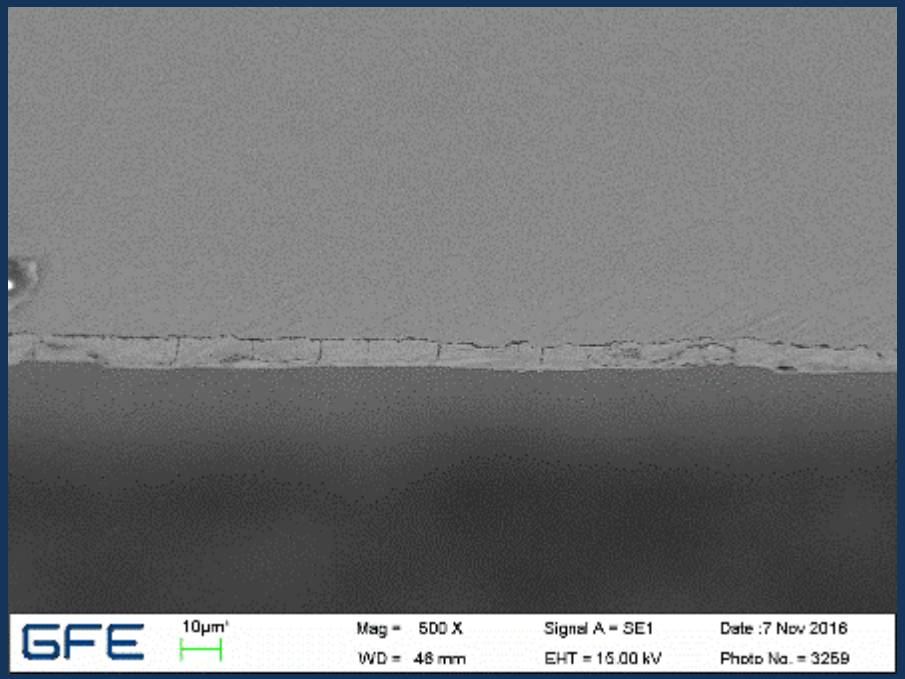

1.5 mm

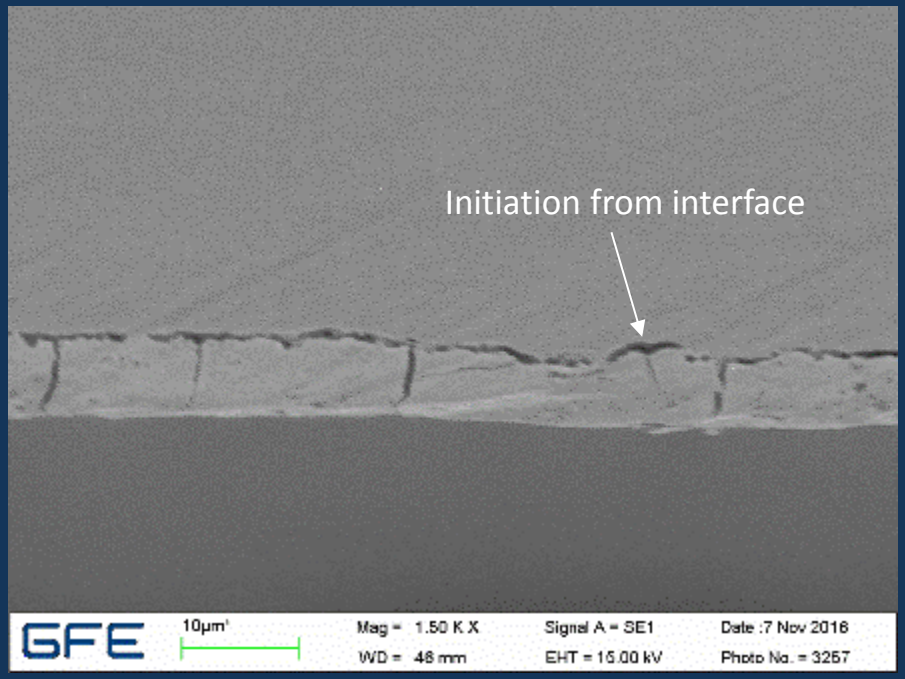

1.5 mm

GA DP980

III

Formability and failure characterization

Modified In-situ bending test in LC-SEM

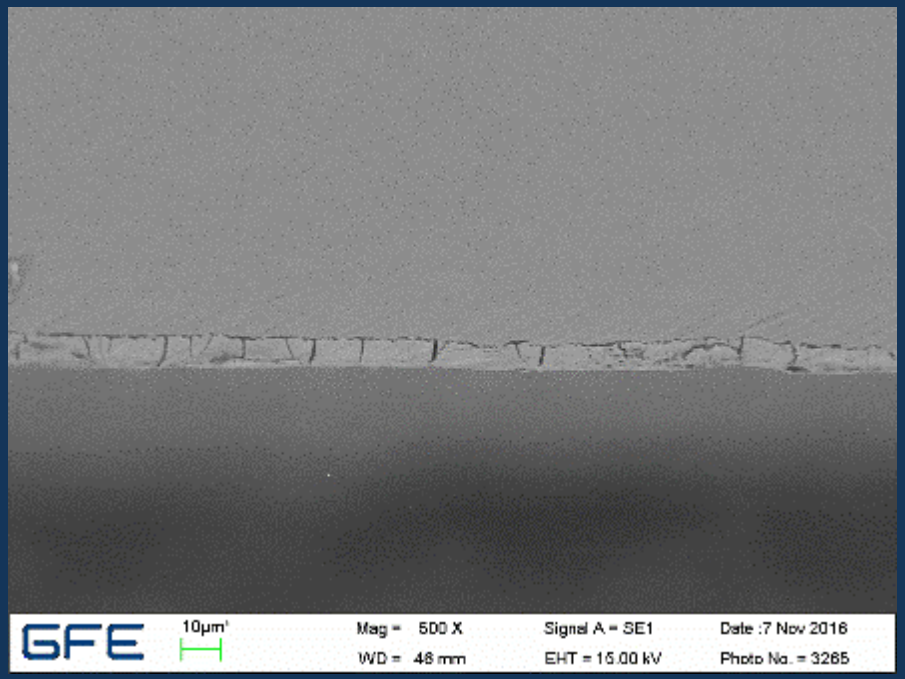

2 mm

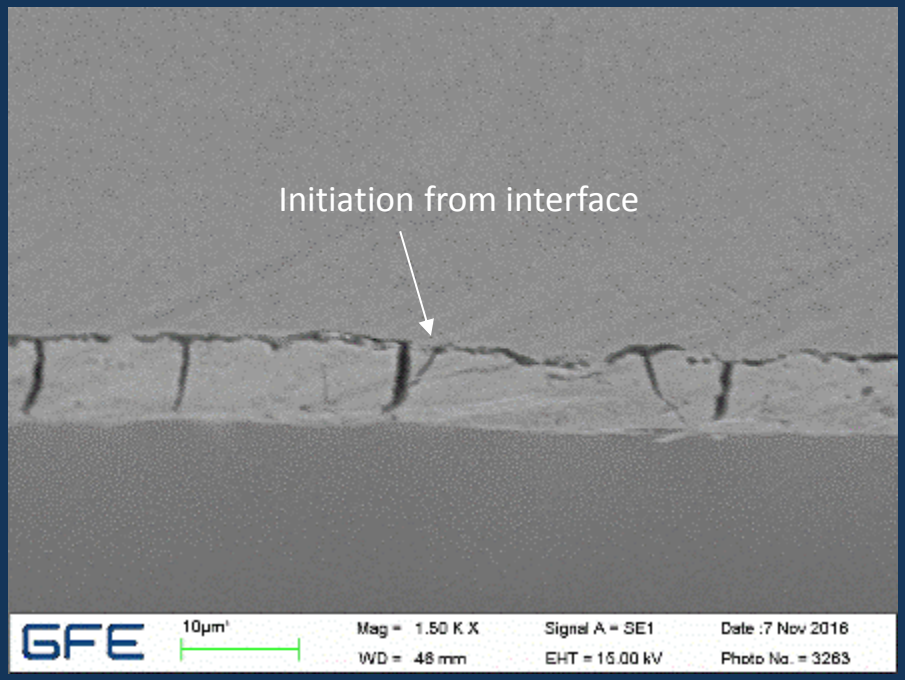

2 mm

GA DP980

III

Formability and failure characterization

Modified In-situ bending test in LC-SEM

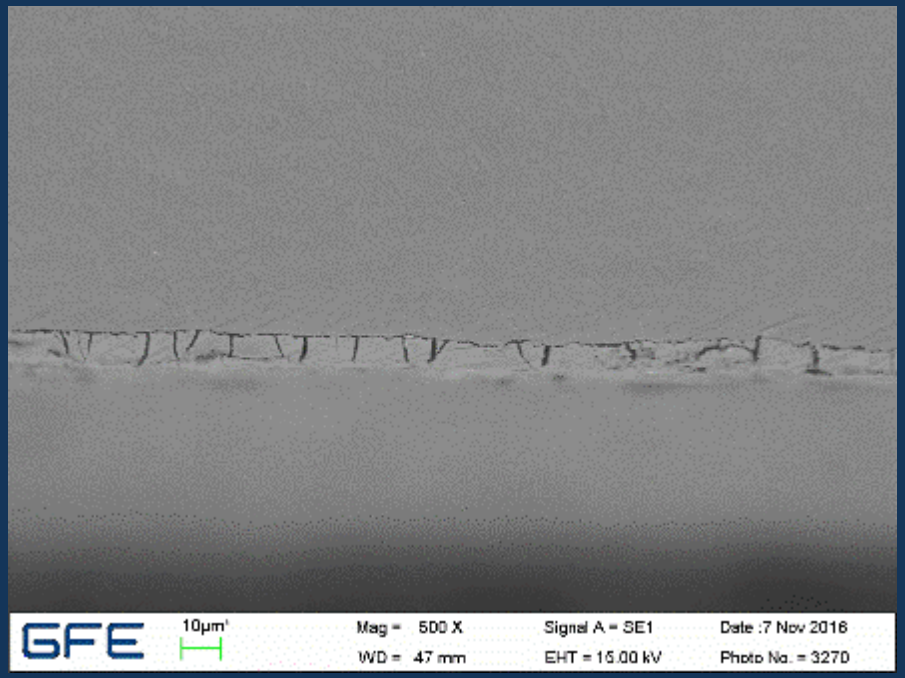

3 mm

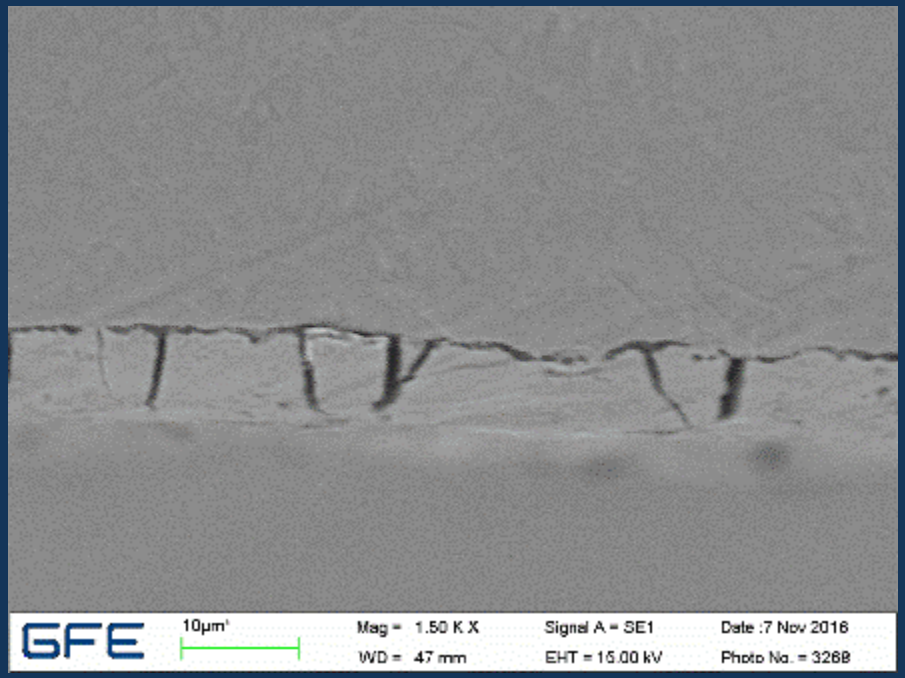

3 mm

GA DP980

III

Formability and failure characterization

Modified In-situ bending test in LC-SEM

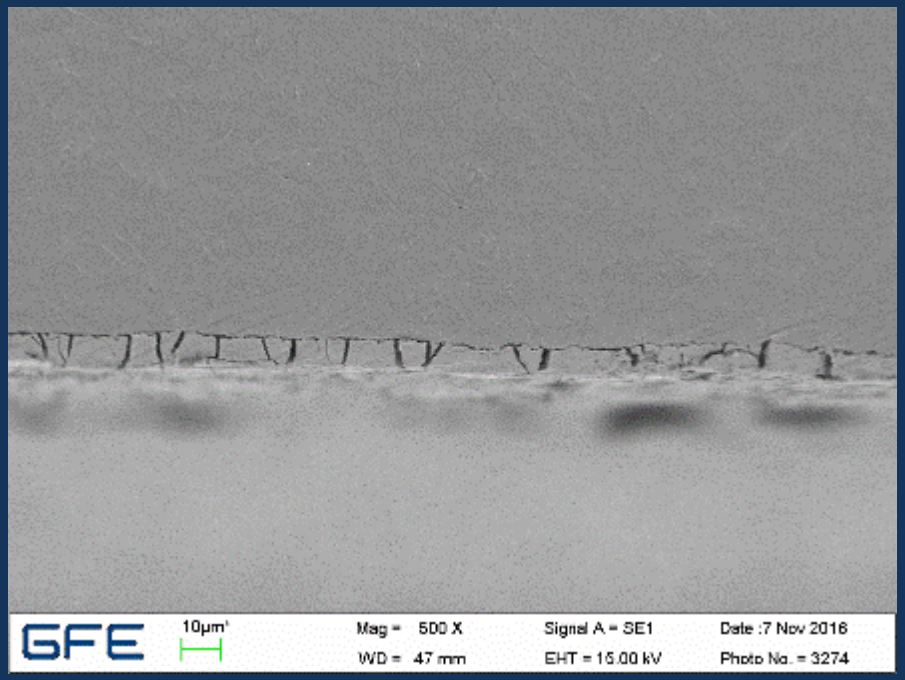

4mm

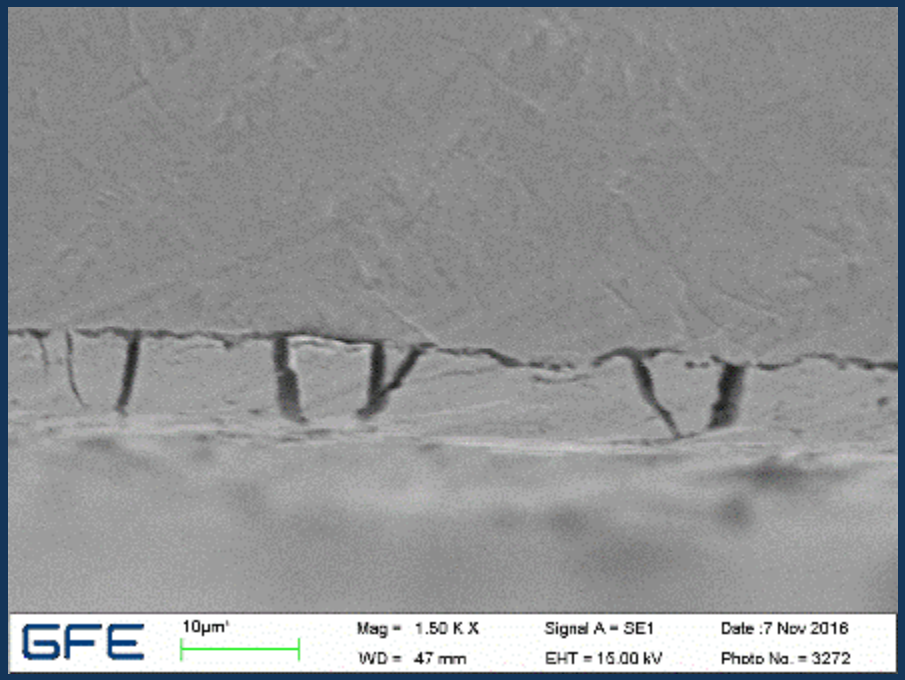

4 mm

GA DP980

III

Formability and failure characterization

Modified In-situ bending test in LC-SEM

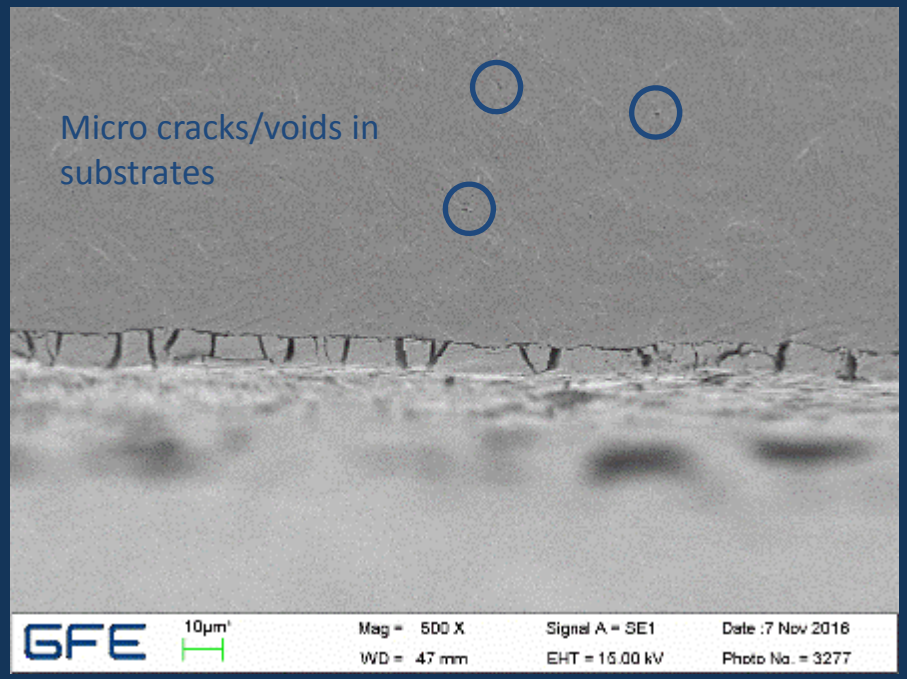

5mm

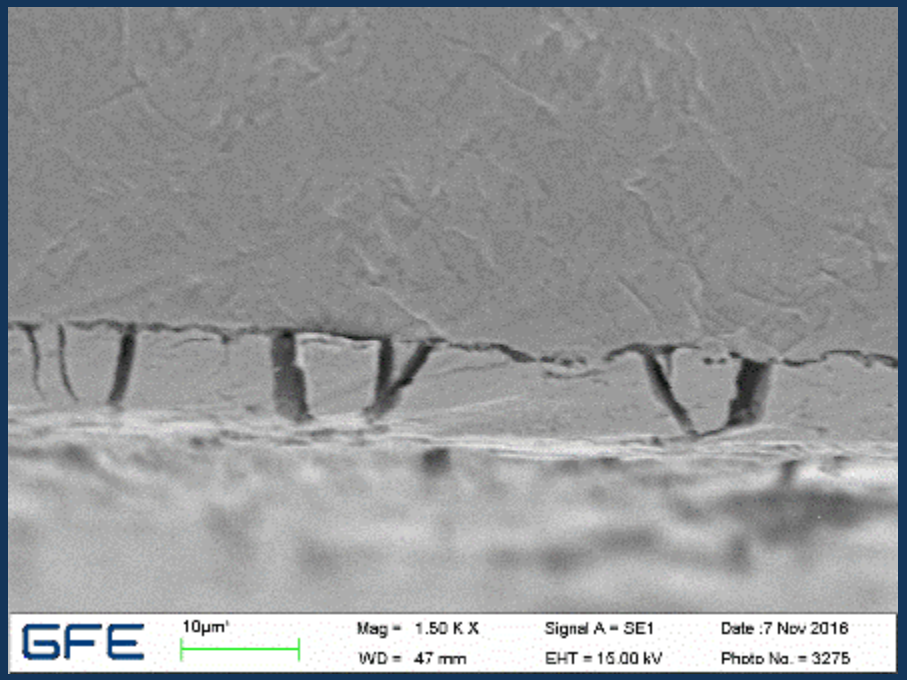

5 mm

GA DP980

III

Formability and failure characterization

Modified In-situ bending test in LC-SEM

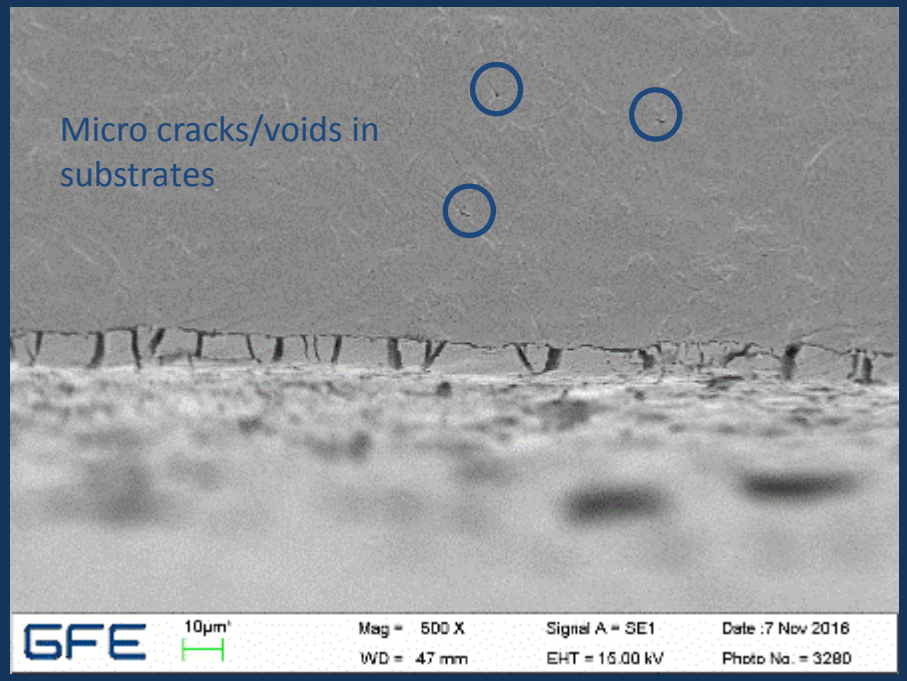

6mm

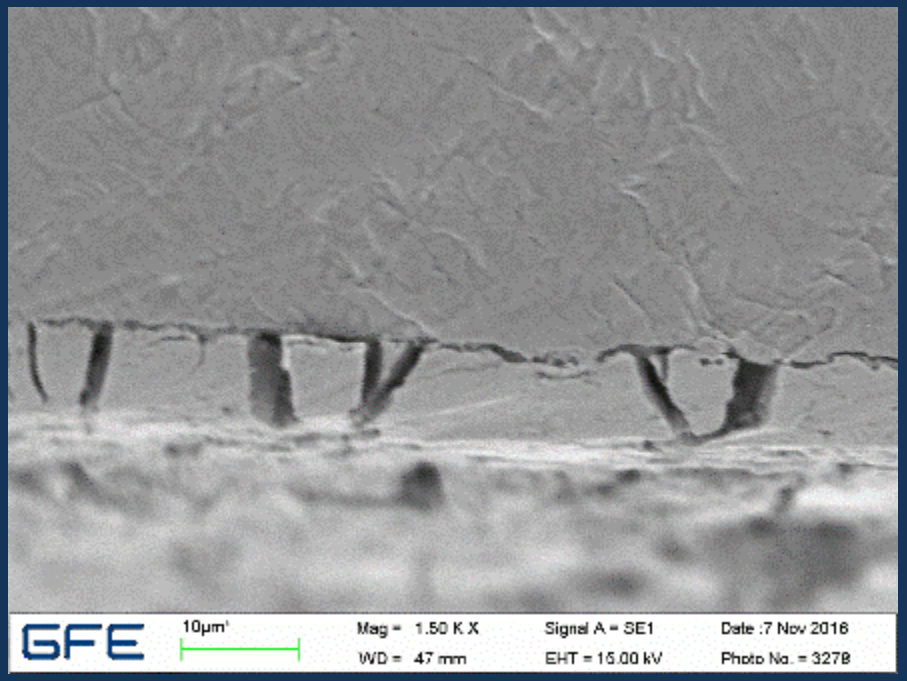

6 mm

GA DP980

III

Formability and failure characterization

Modified In-situ bending test in LC-SEM

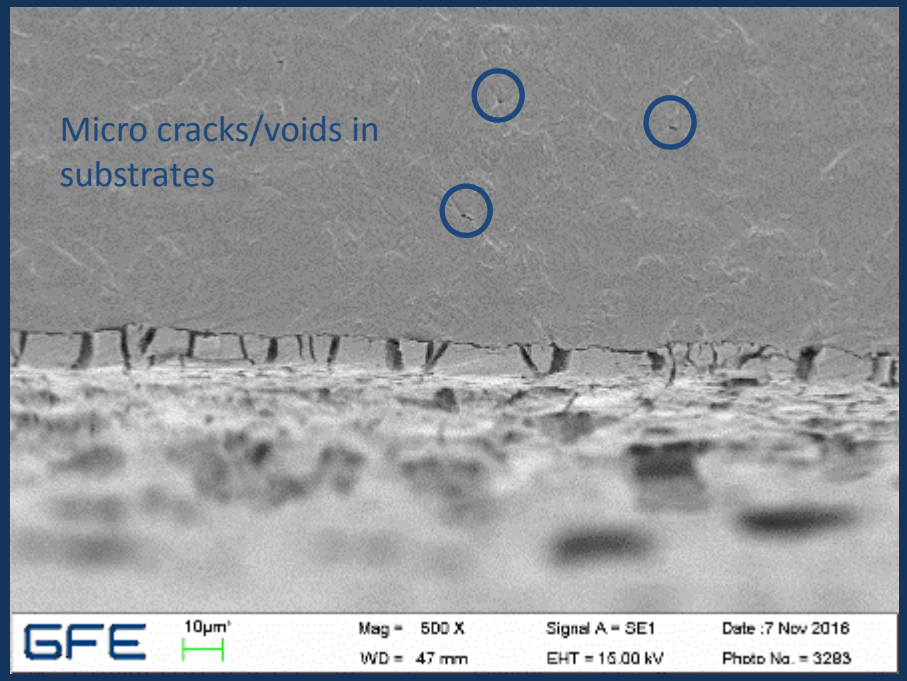

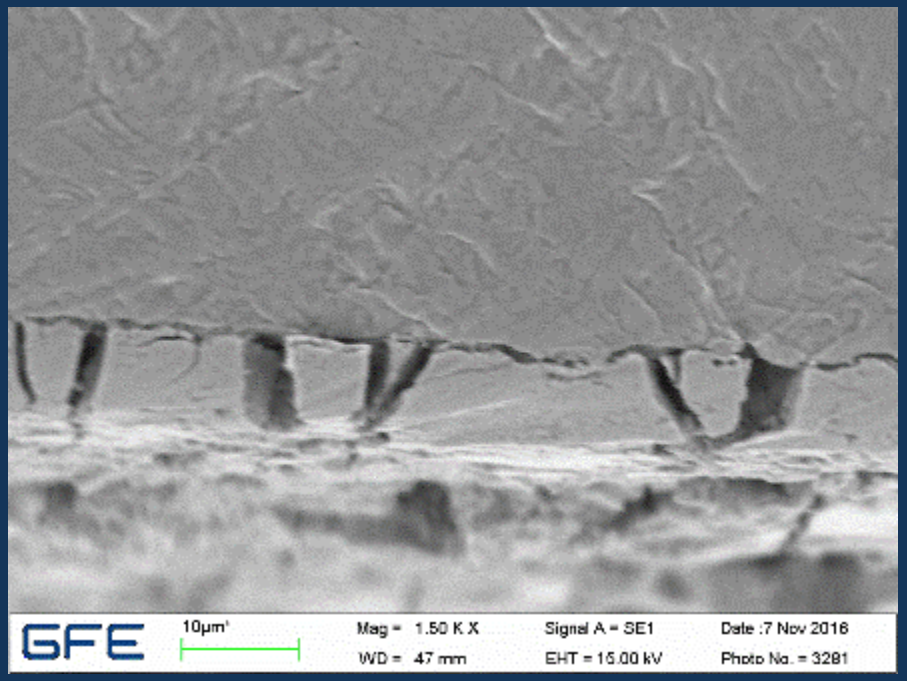

7mm

7 mm

GA DP980

III

Formability and failure characterization

Modified In-situ bending test in LC-SEM

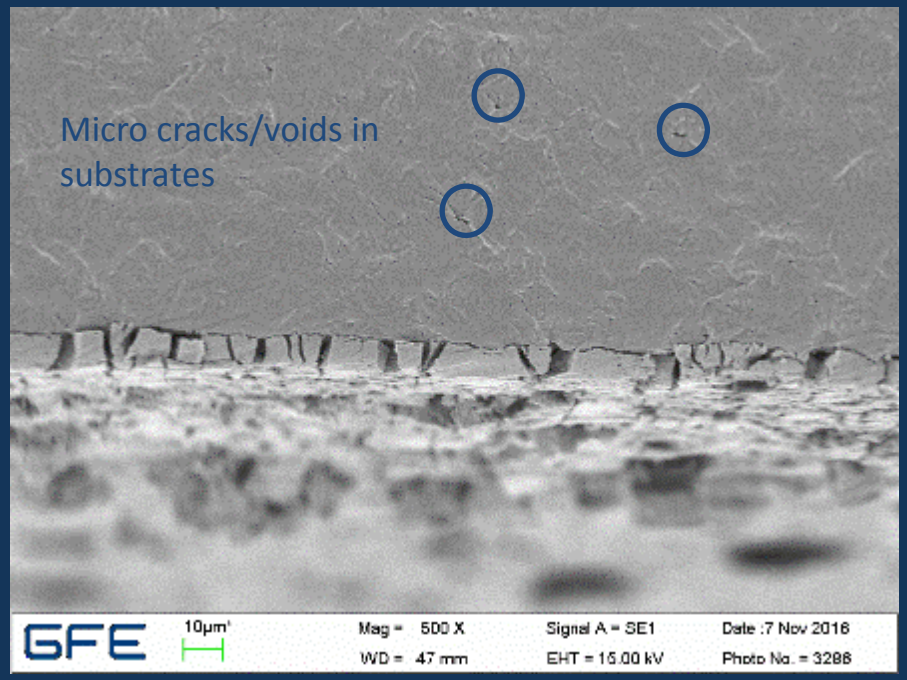

8 mm

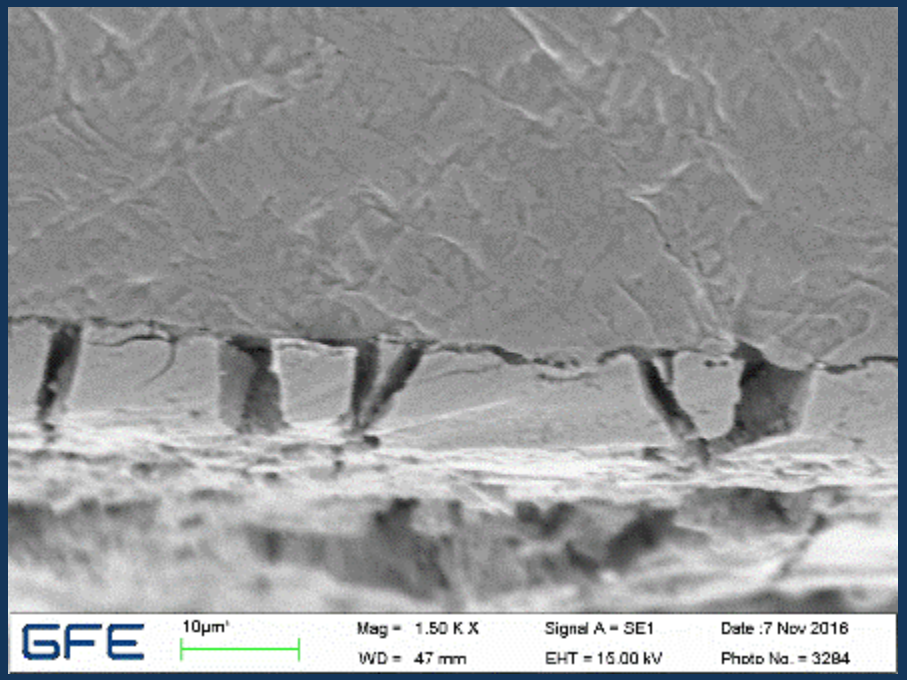

8 mm

GA DP980

III

Formability and failure characterization

Modified In-situ bending test in LC-SEM

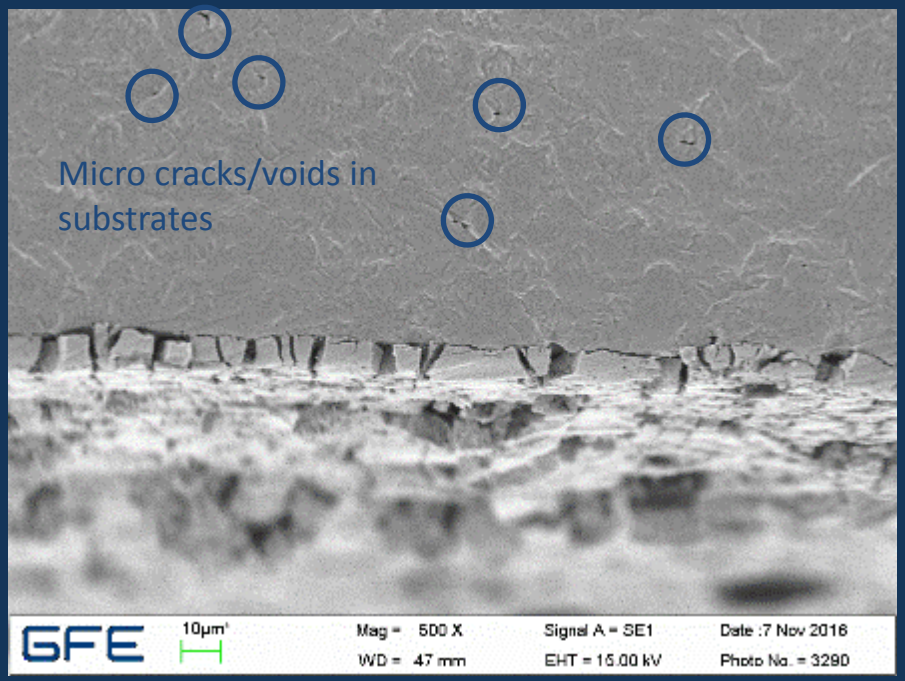

9 mm

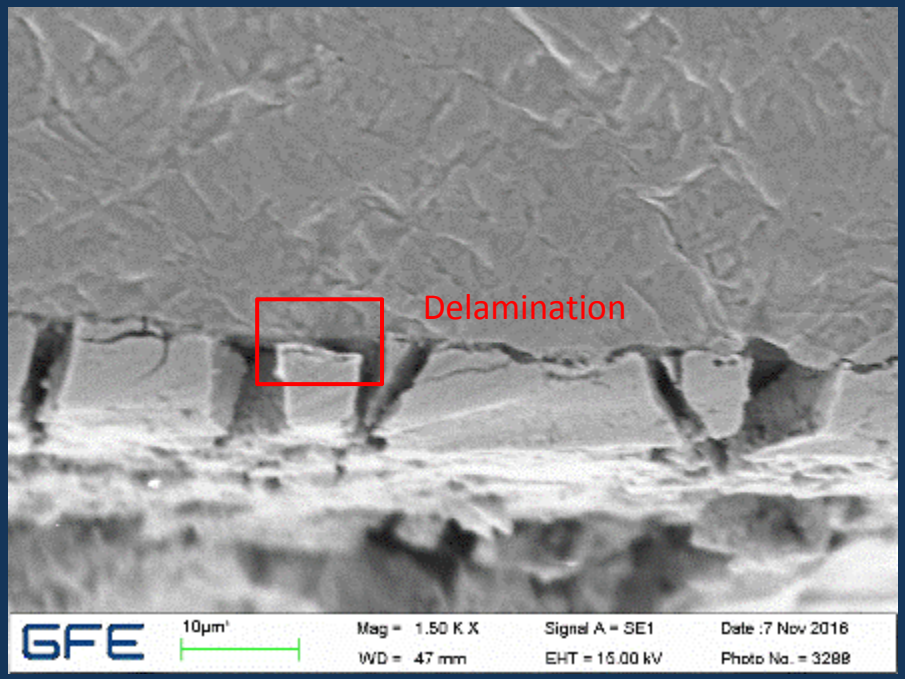

9 mm

GA DP980

III

Formability and failure characterization

Modified In-situ bending test in LC-SEM

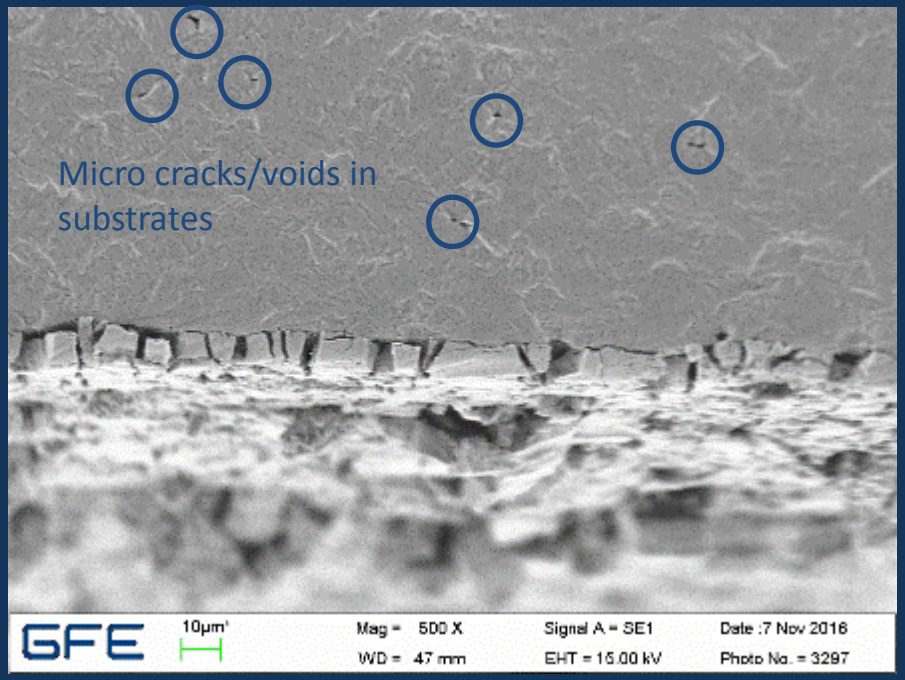

10 mm

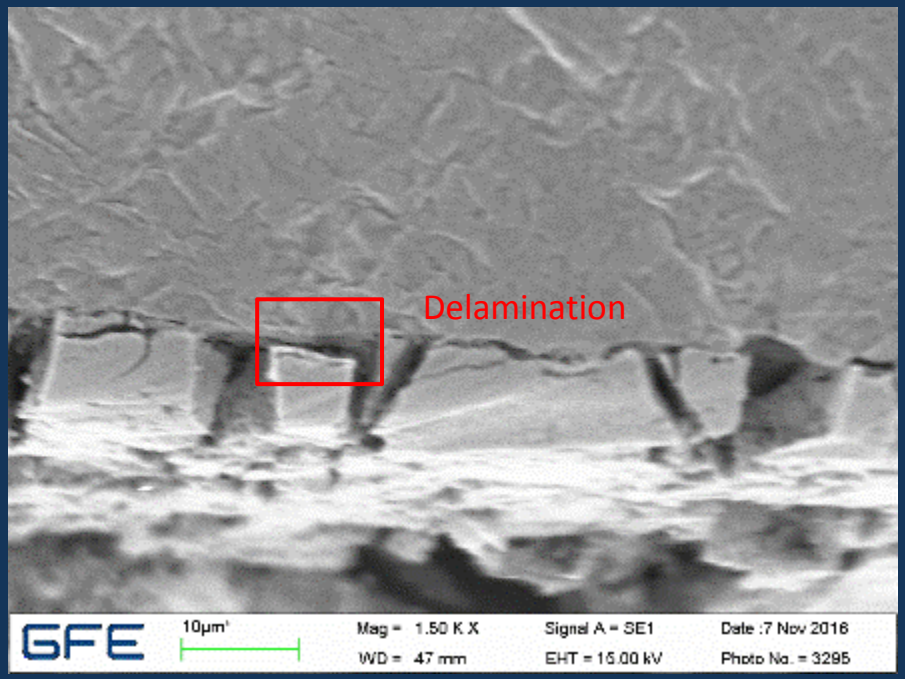

10 mm

GA DP980

III

Formability and failure characterization

Modified In-situ bending test in LC-SEM

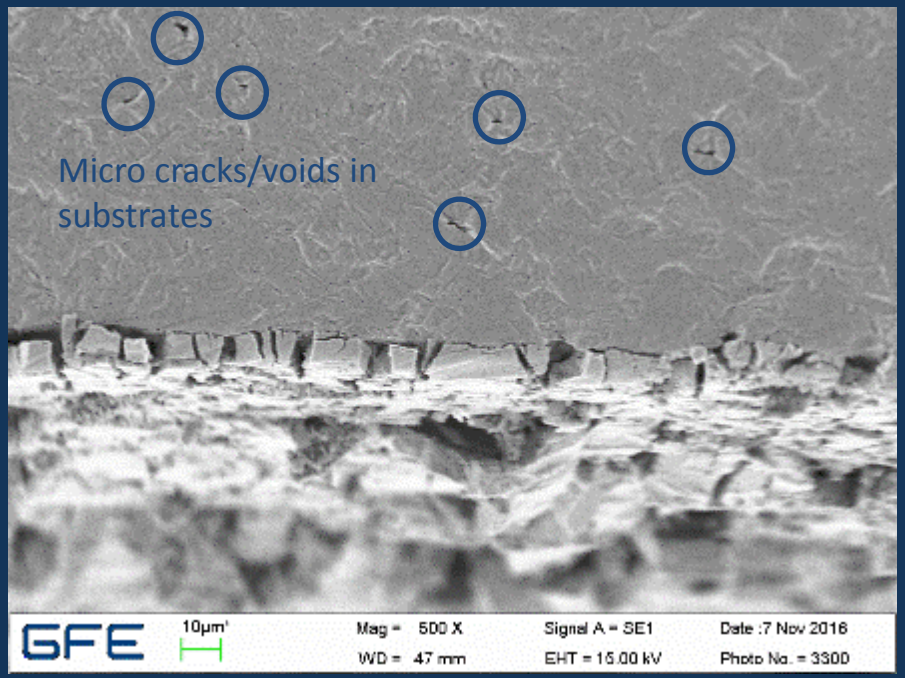

11 mm

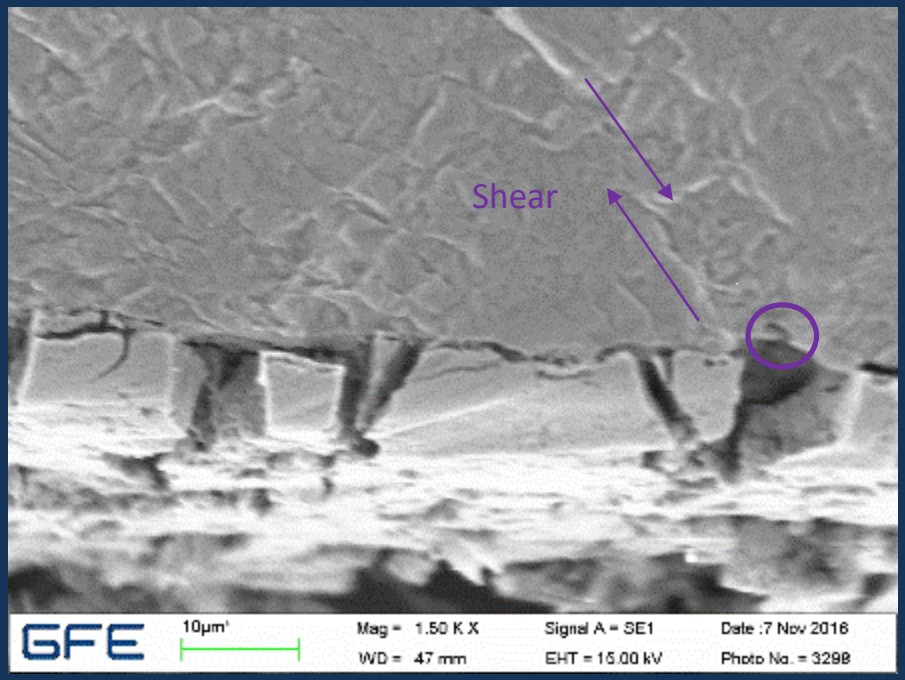

11 mm

GA DP980

III

Formability and failure characterization

Modified In-situ bending test in LC-SEM

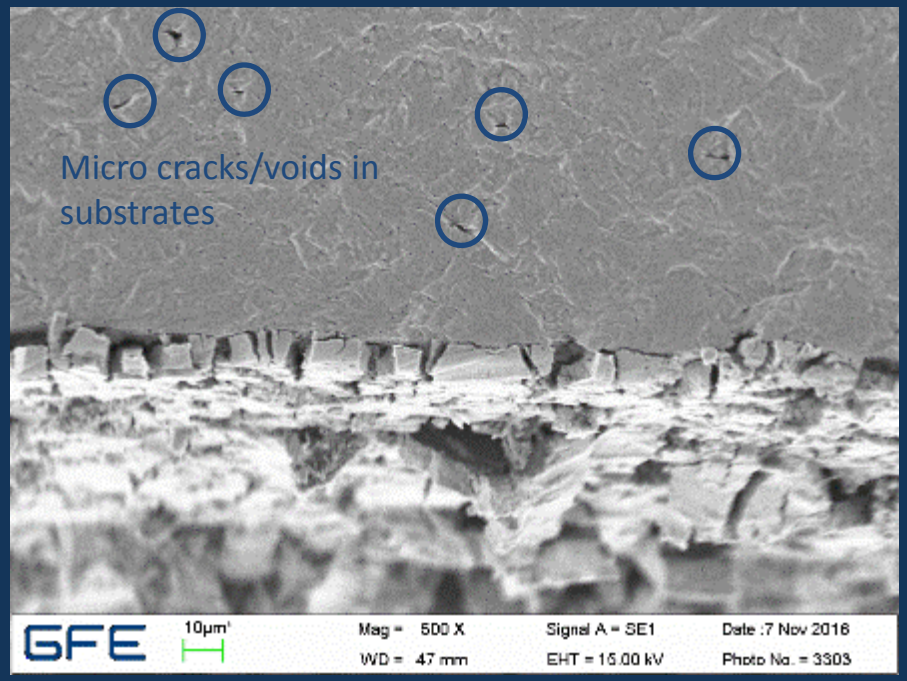

12 mm

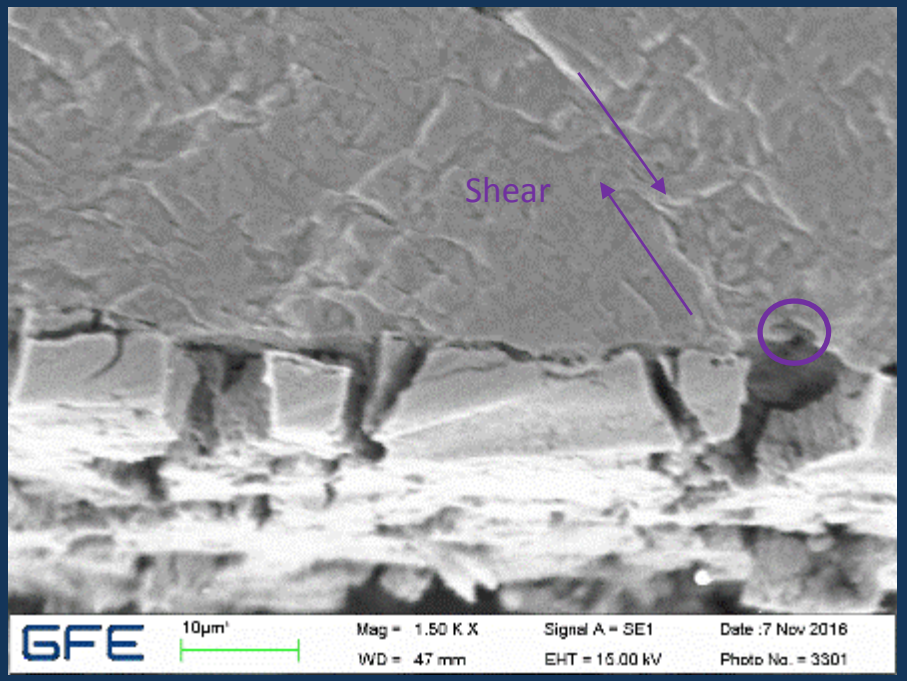

12 mm

GA DP980

III

Formability and failure characterization

Modified In-situ bending test in LC-SEM

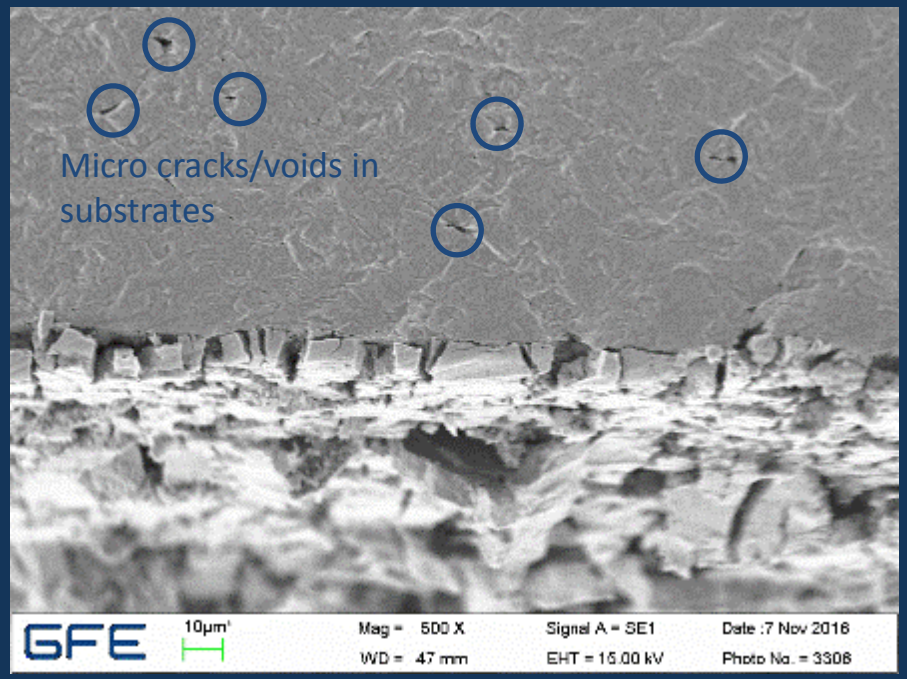

13 mm

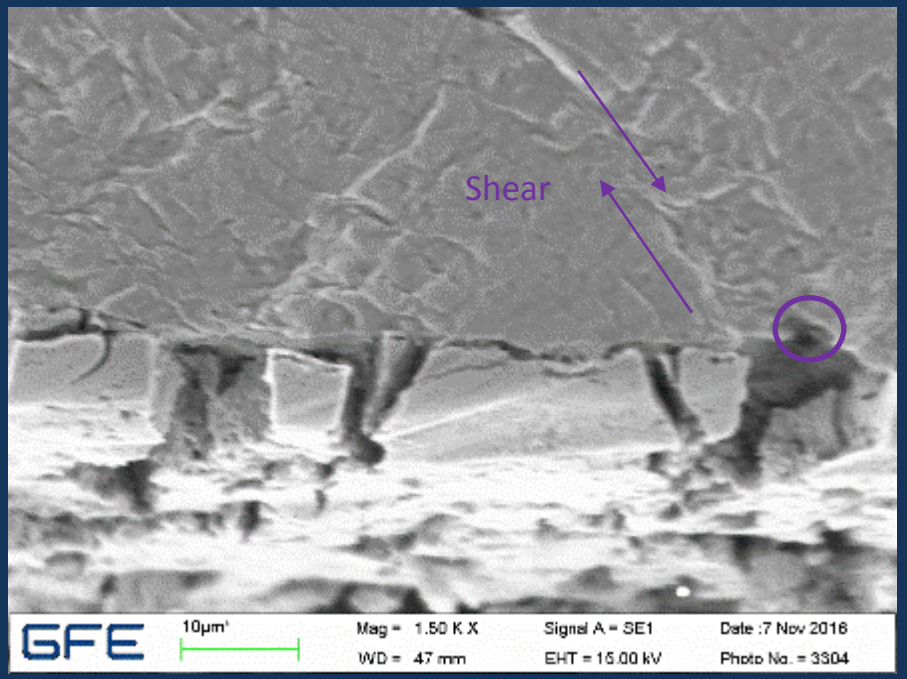

13 mm

GA DP980

III

Formability and failure characterization

Modified In-situ bending test in LC-SEM

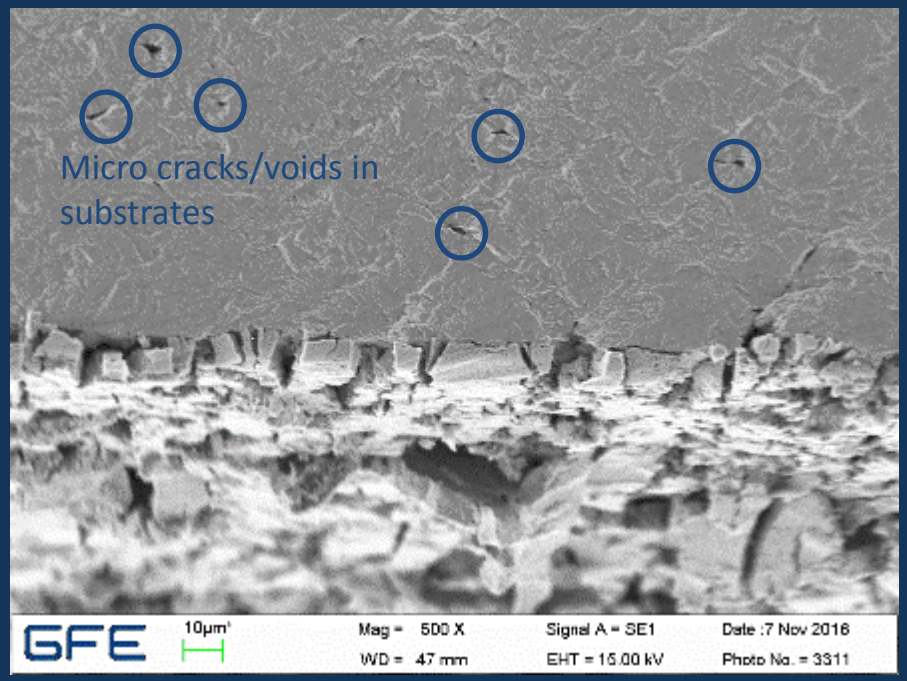

14 mm

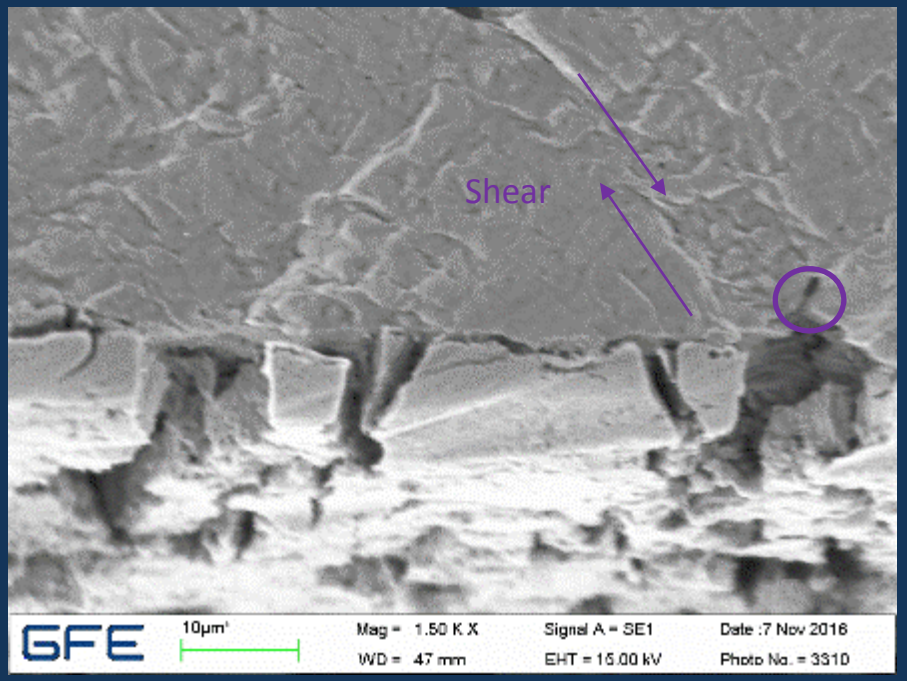

14 mm

GA DP980

Modified In-situ bending test in LC-SEM

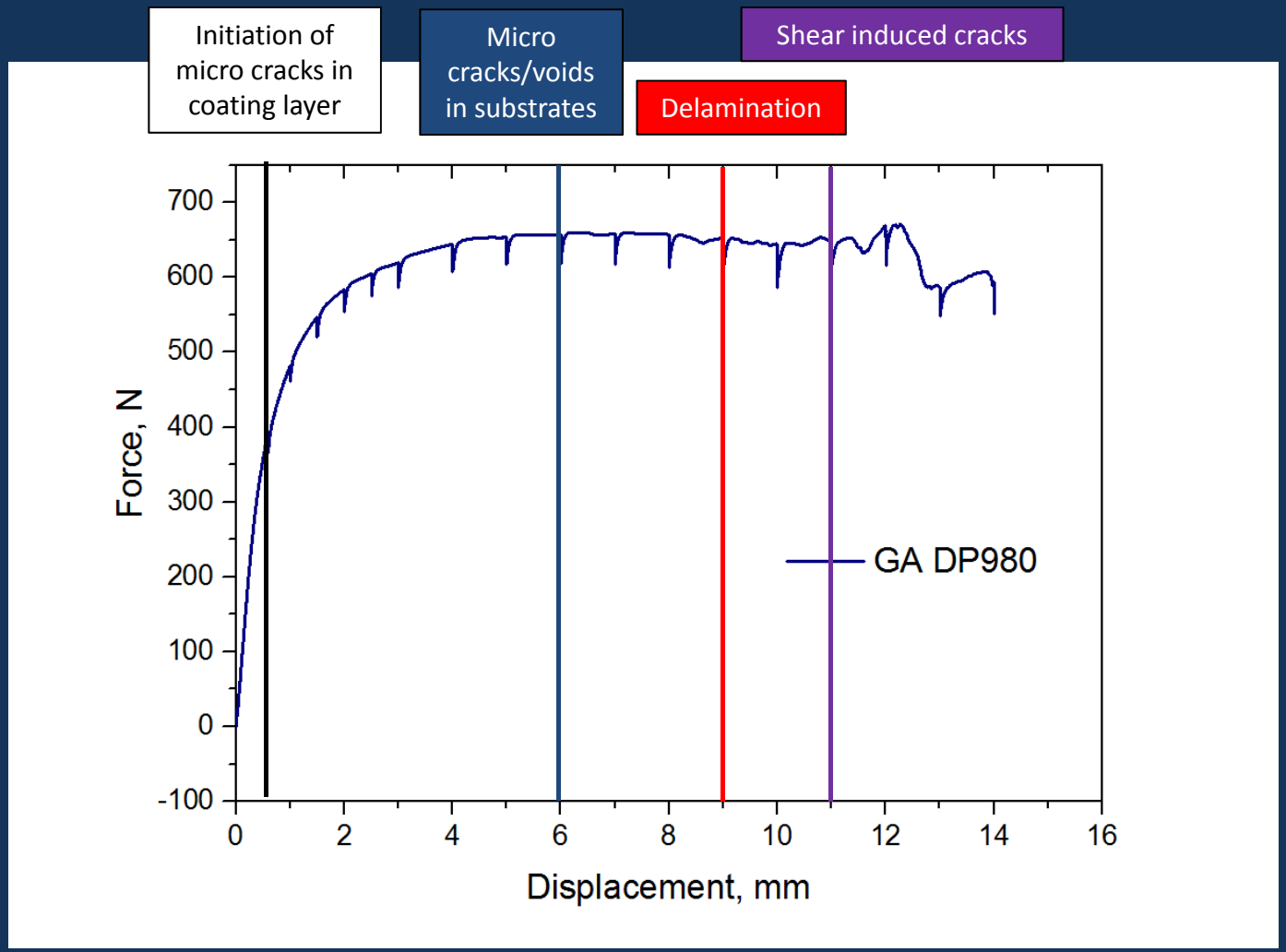

Formability and failure characterization

Modified In-situ bending test in LC-SEM

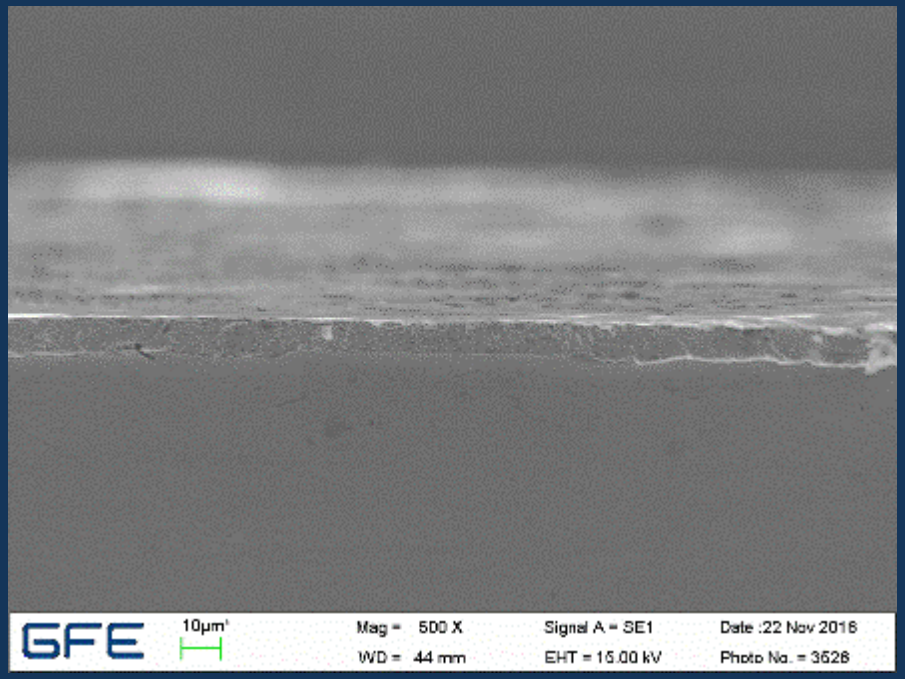

0 mm

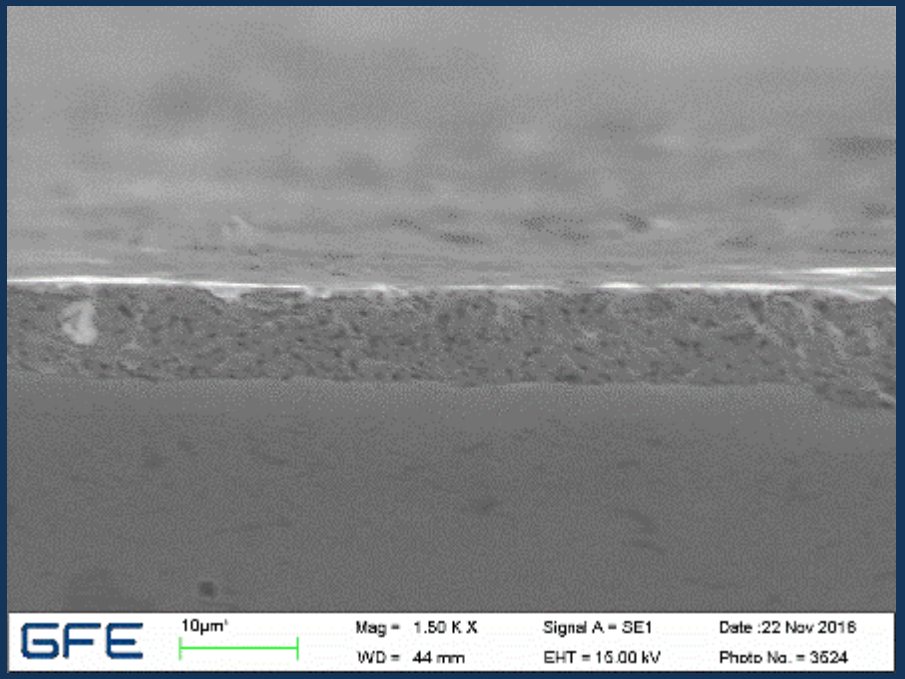

0 mm

EG DP980

Formability and failure characterization

Modified In-situ bending test in LC-SEM

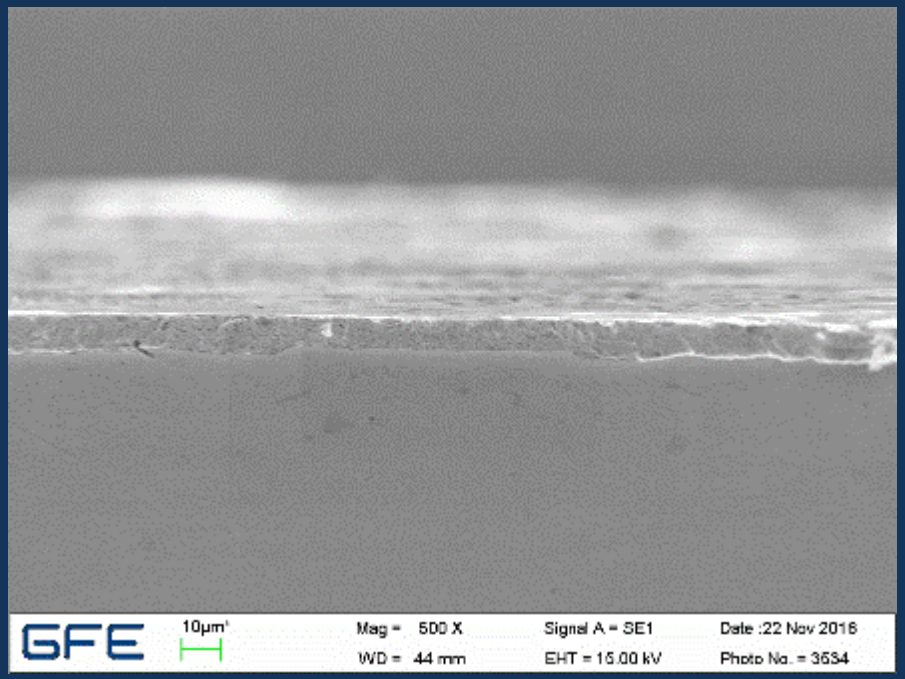

1mm

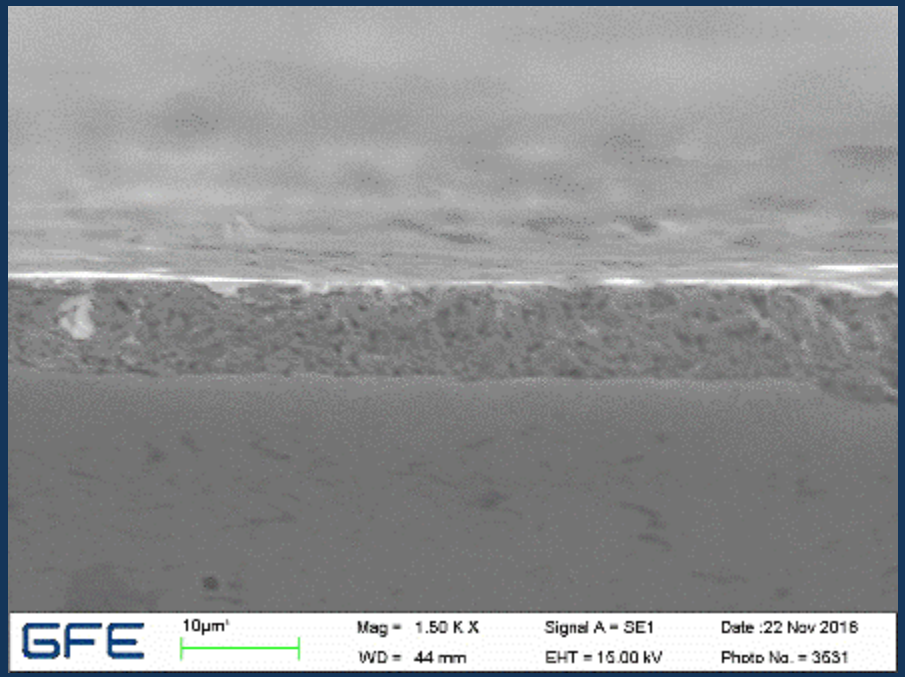

1 mm

EG DP980

Formability and failure characterization

Modified In-situ bending test in LC-SEM

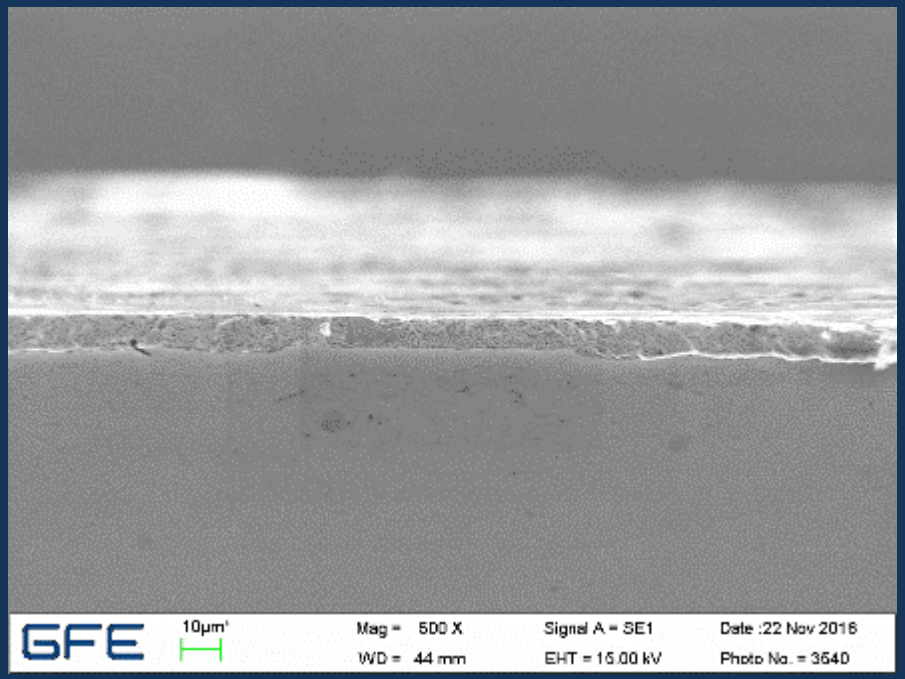

2 mm

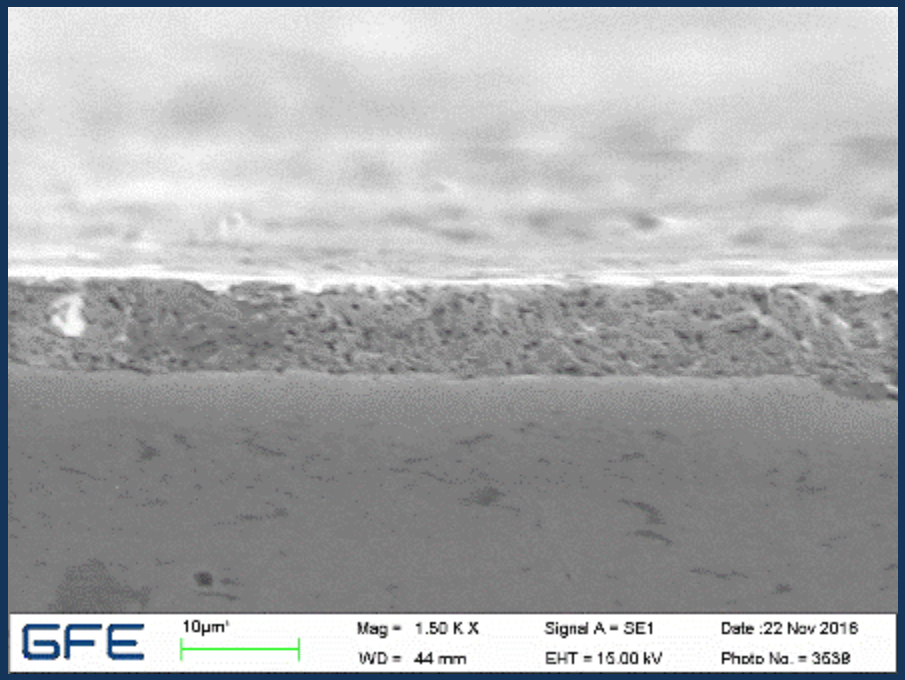

2 mm

EG DP980

Formability and failure characterization

Modified In-situ bending test in LC-SEM

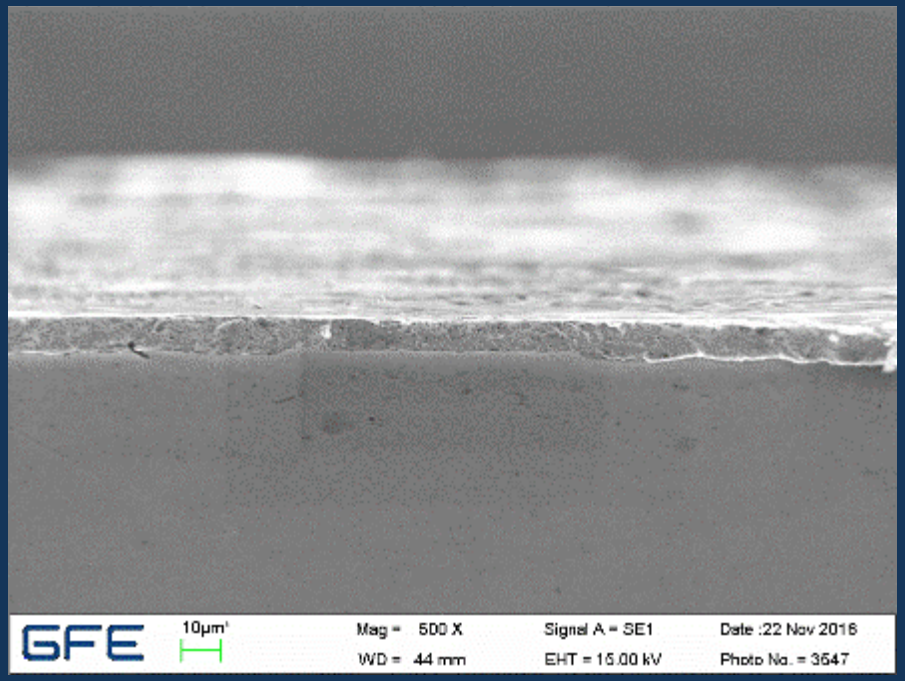

3 mm

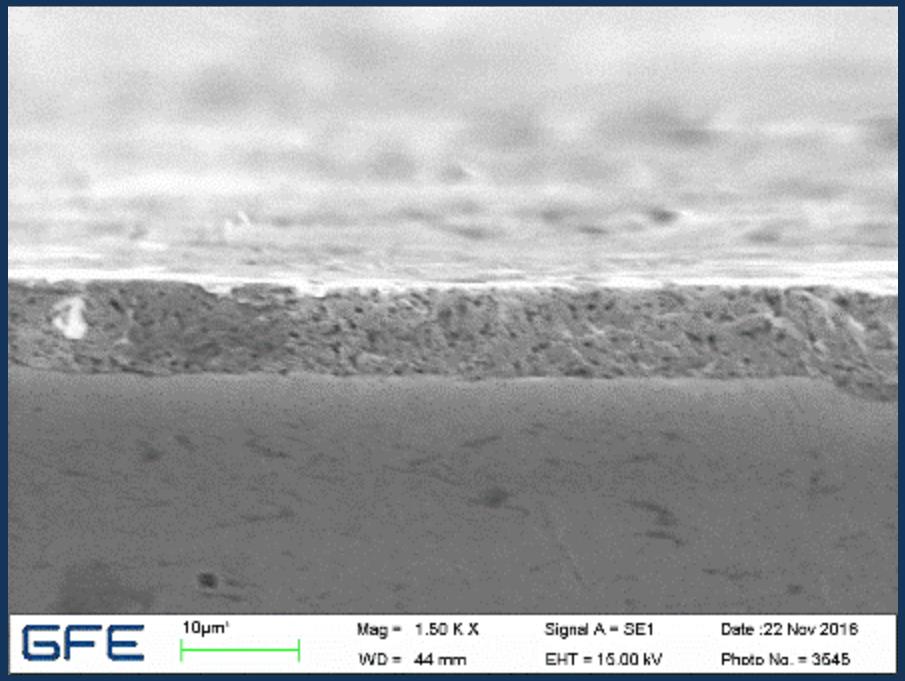

3 mm

EG DP980

Formability and failure characterization

Modified In-situ bending test in LC-SEM

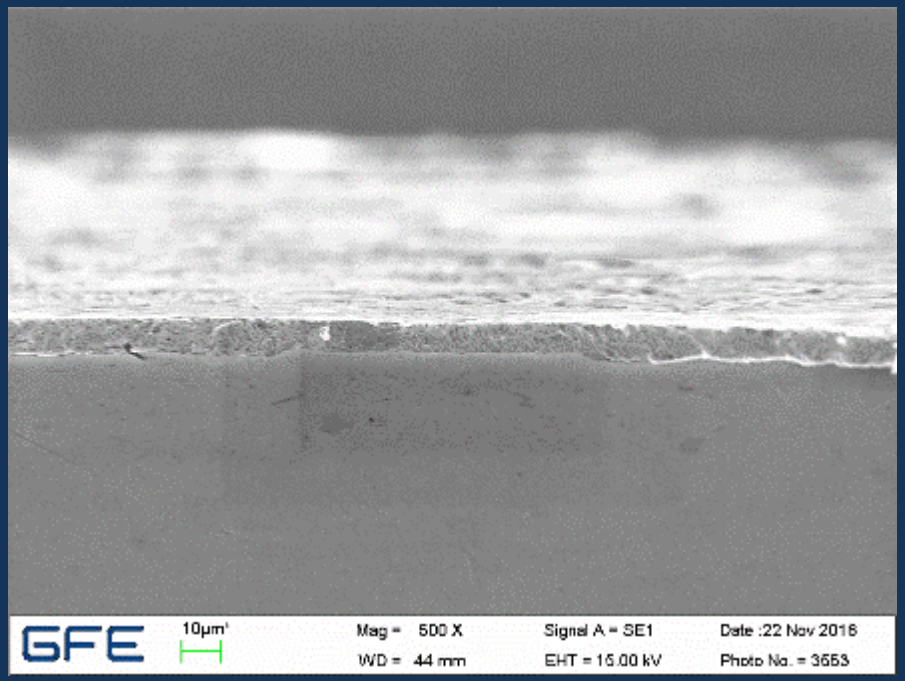

4 mm

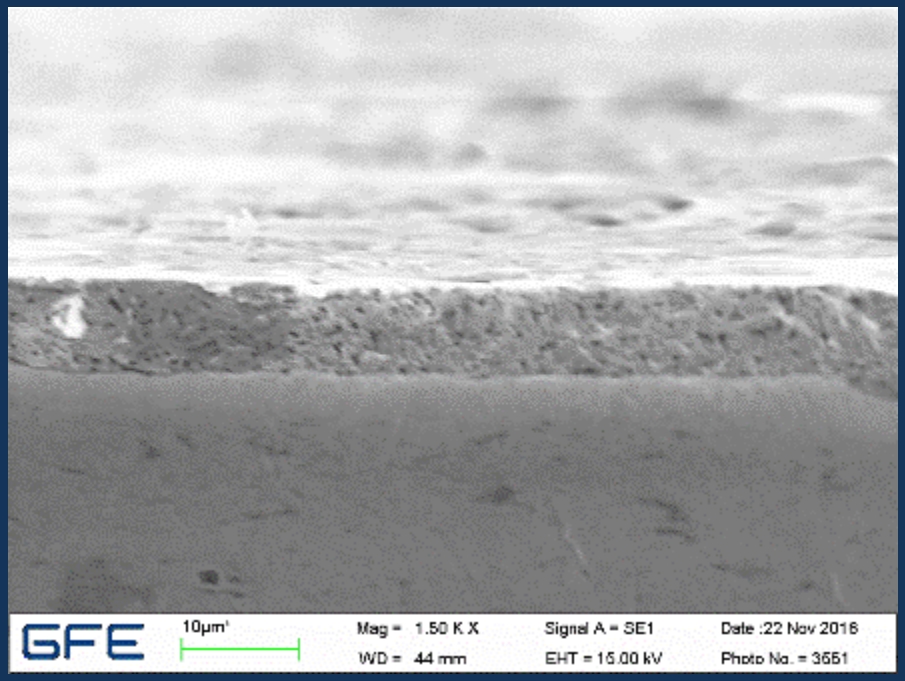

4 mm

EG DP980

Formability and failure characterization

Modified In-situ bending test in LC-SEM

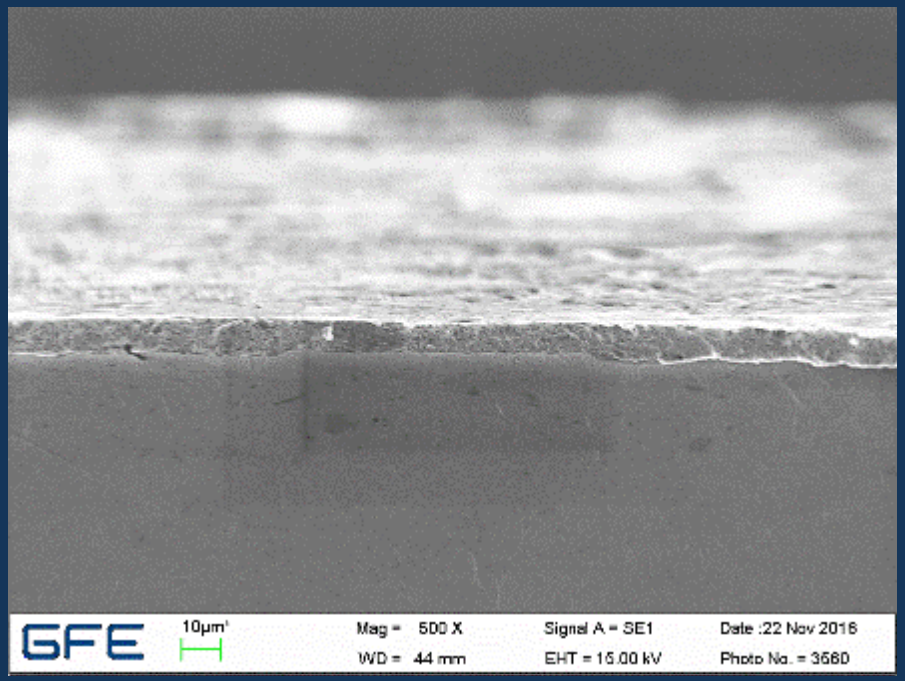

5 mm

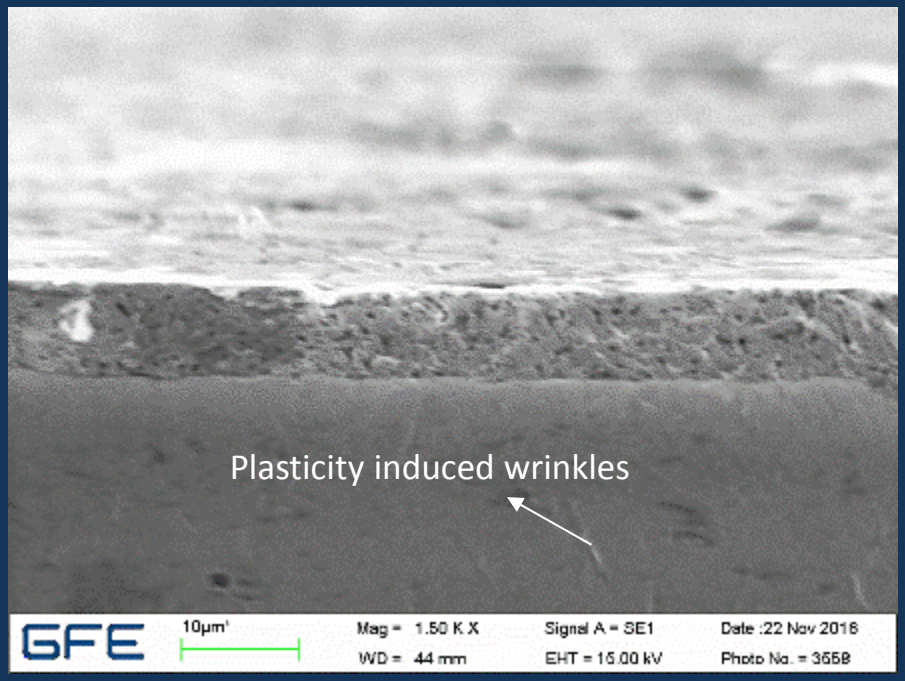

5 mm

EG DP980

Formability and failure characterization

Modified In-situ bending test in LC-SEM

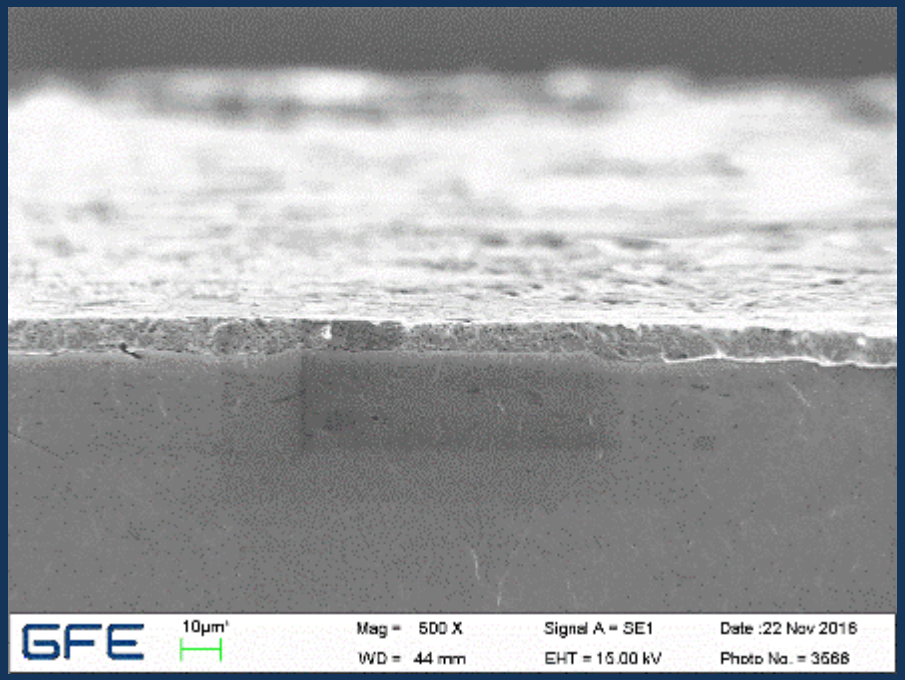

6 mm

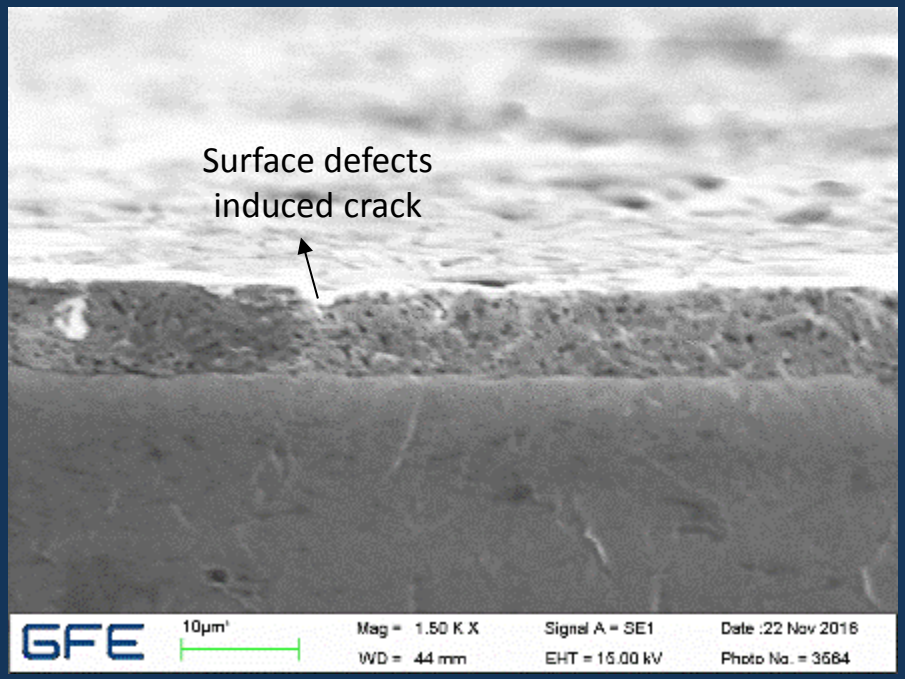

6 mm

EG DP980

Formability and failure characterization

Modified In-situ bending test in LC-SEM

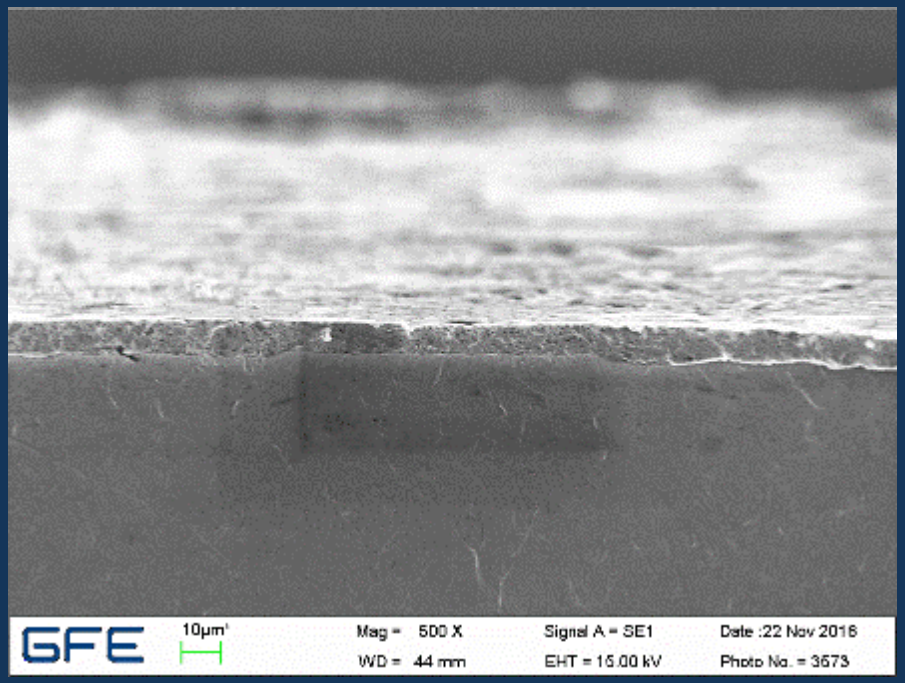

7 mm

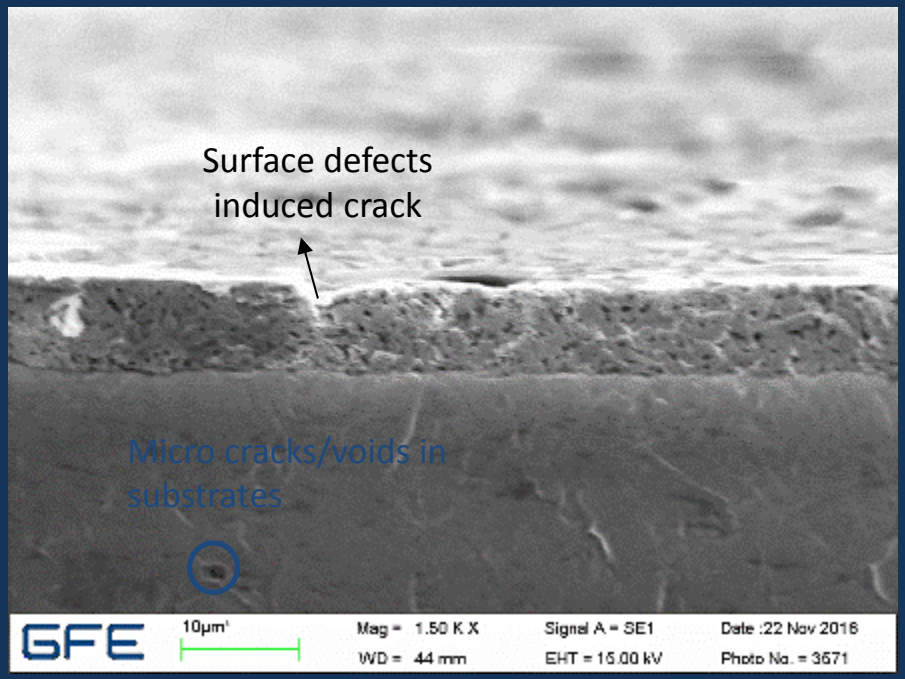

7 mm

EG DP980

Formability and failure characterization

Modified In-situ bending test in LC-SEM

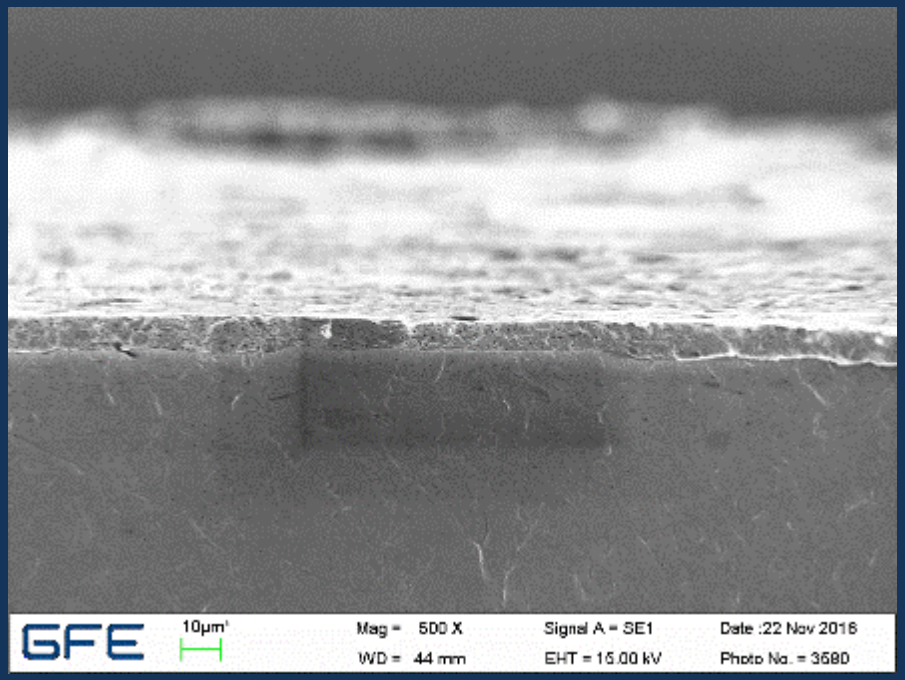

8 mm

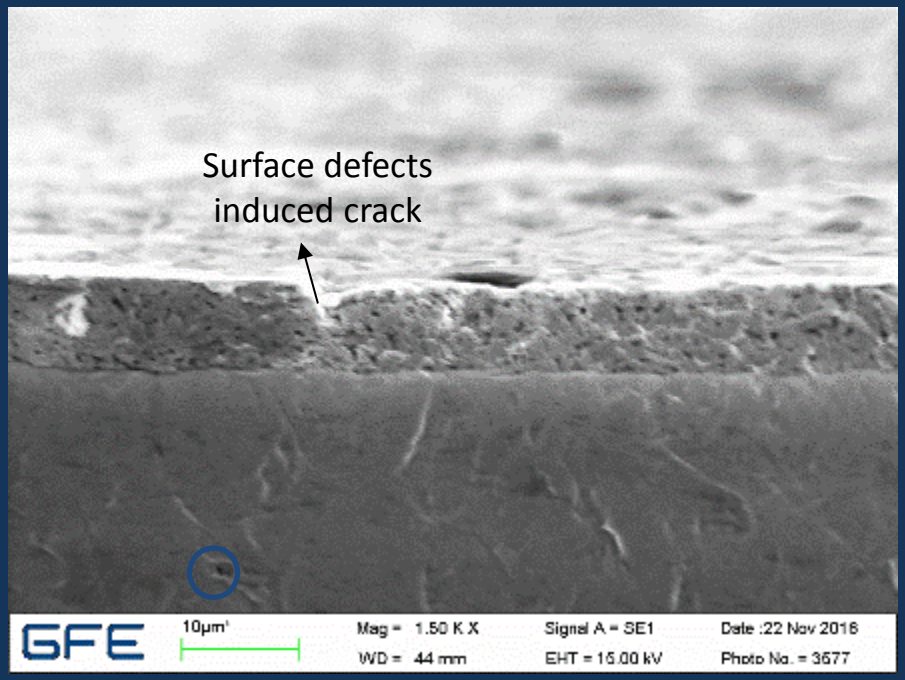

8 mm

EG DP980

Formability and failure characterization

Modified In-situ bending test in LC-SEM

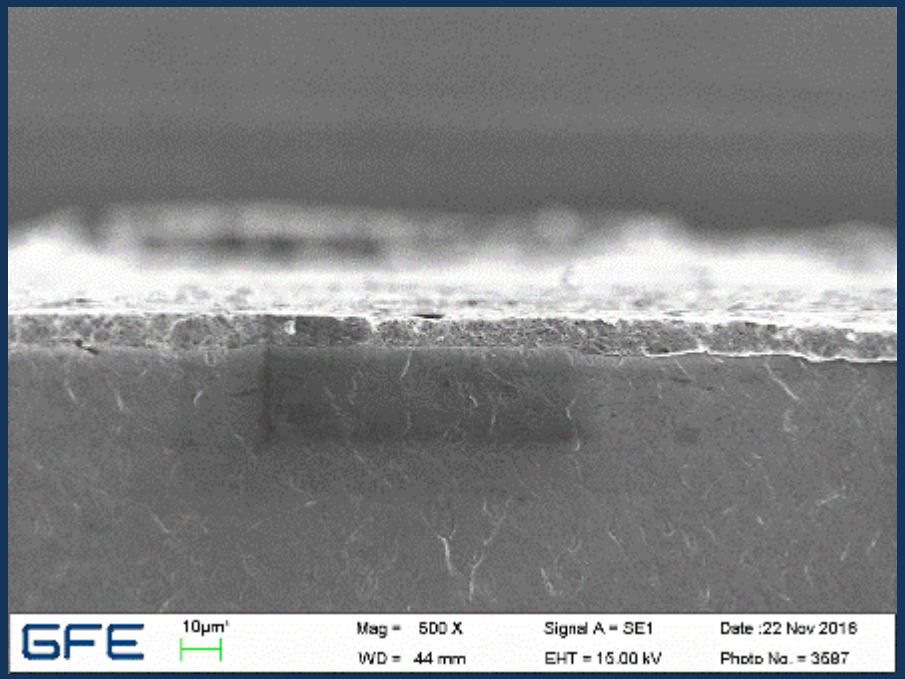

9 mm

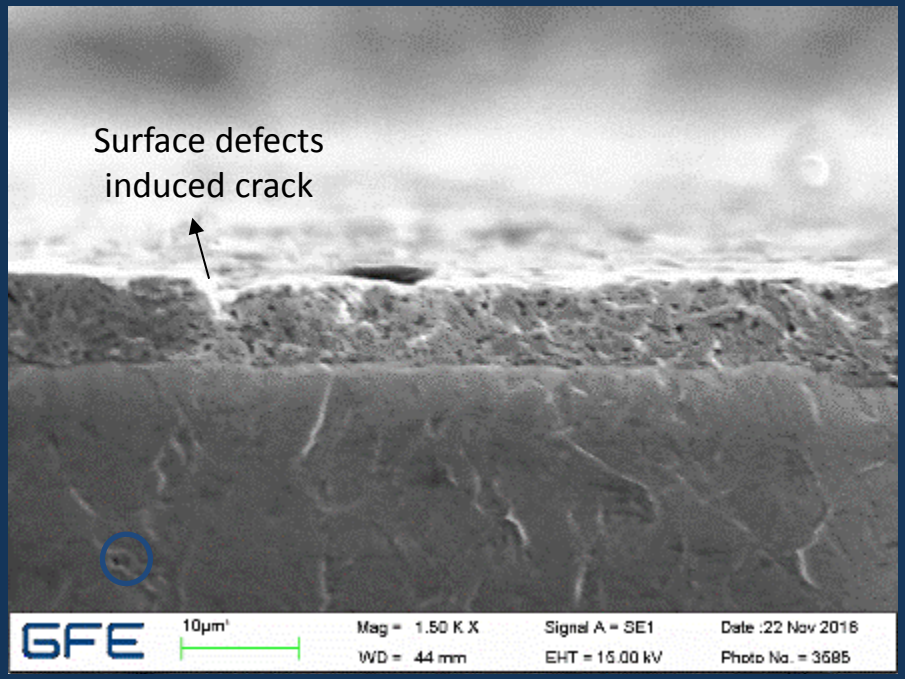

9 mm

EG DP980

Formability and failure characterization

Modified In-situ bending test in LC-SEM

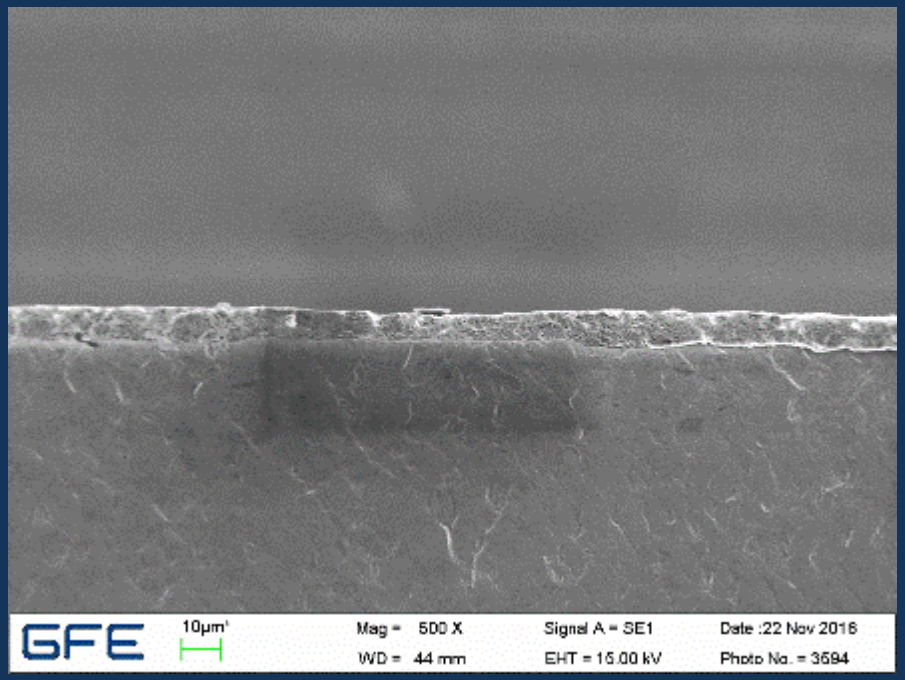

10 mm

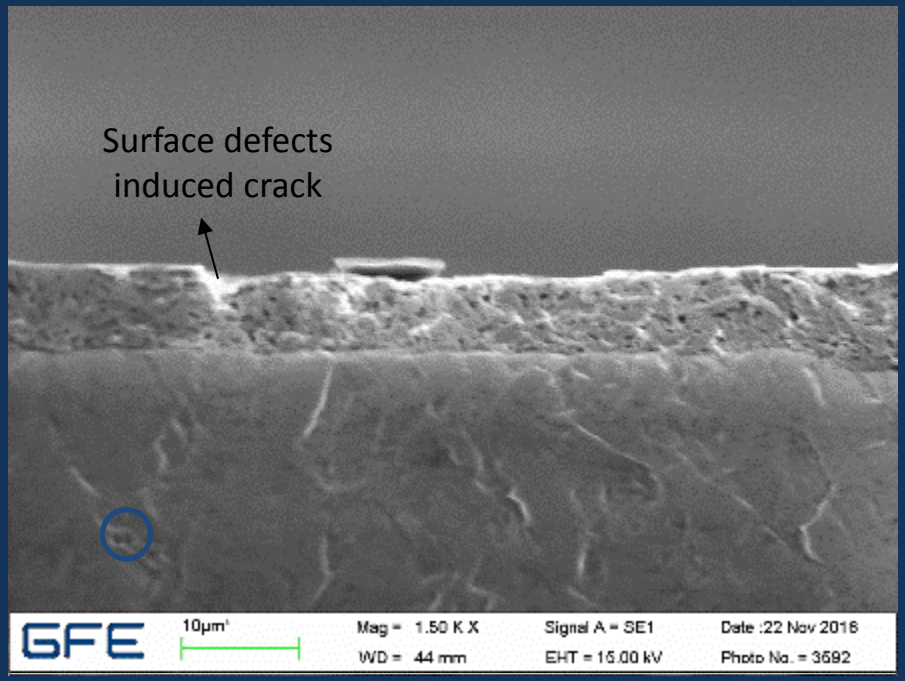

10 mm

EG DP980

Formability and failure characterization

Modified In-situ bending test in LC-SEM

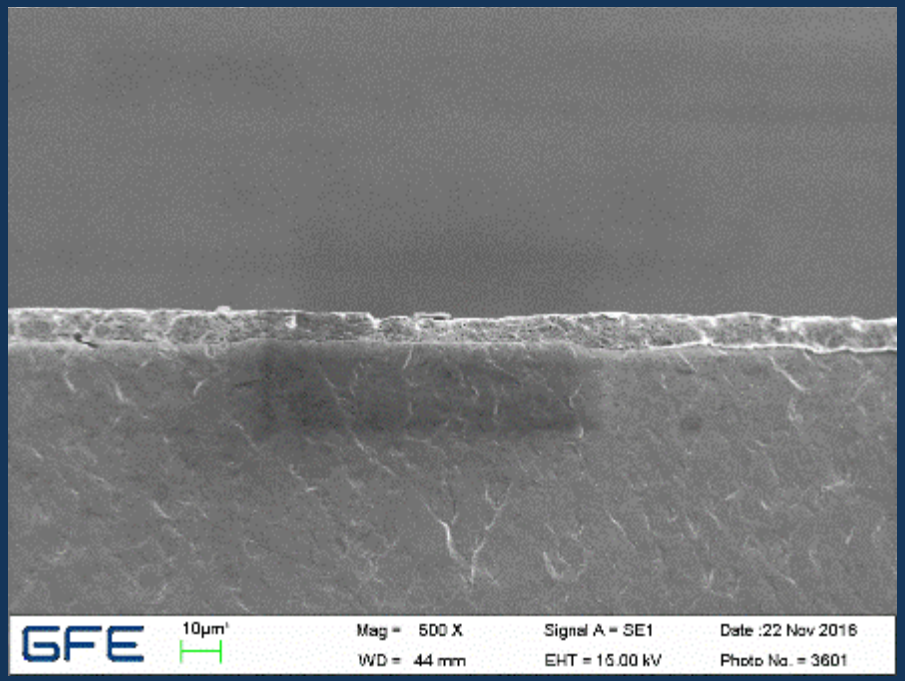

11 mm

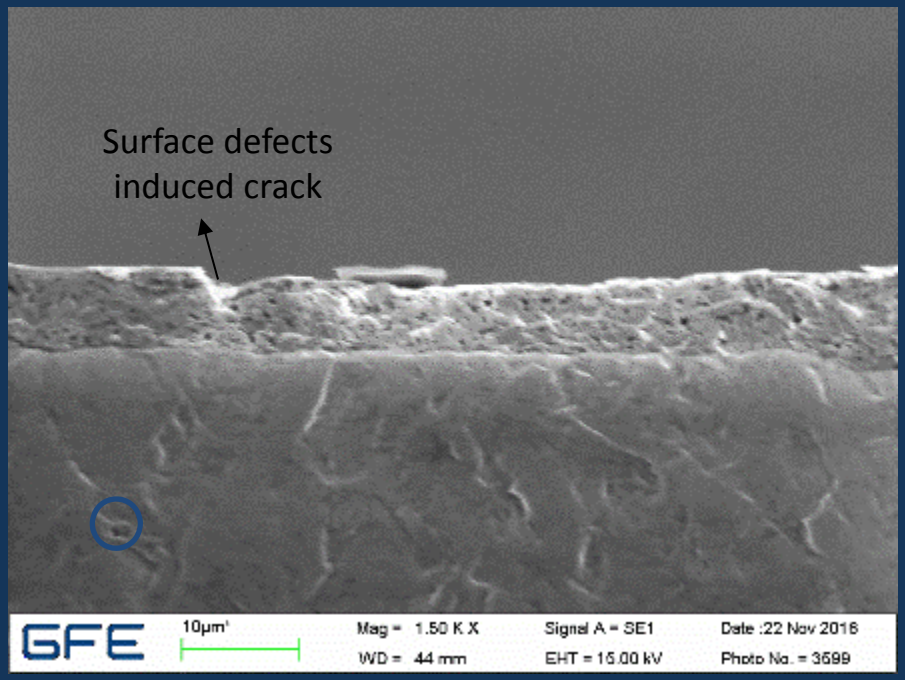

11 mm

EG DP980

Formability and failure characterization

Modified In-situ bending test in LC-SEM

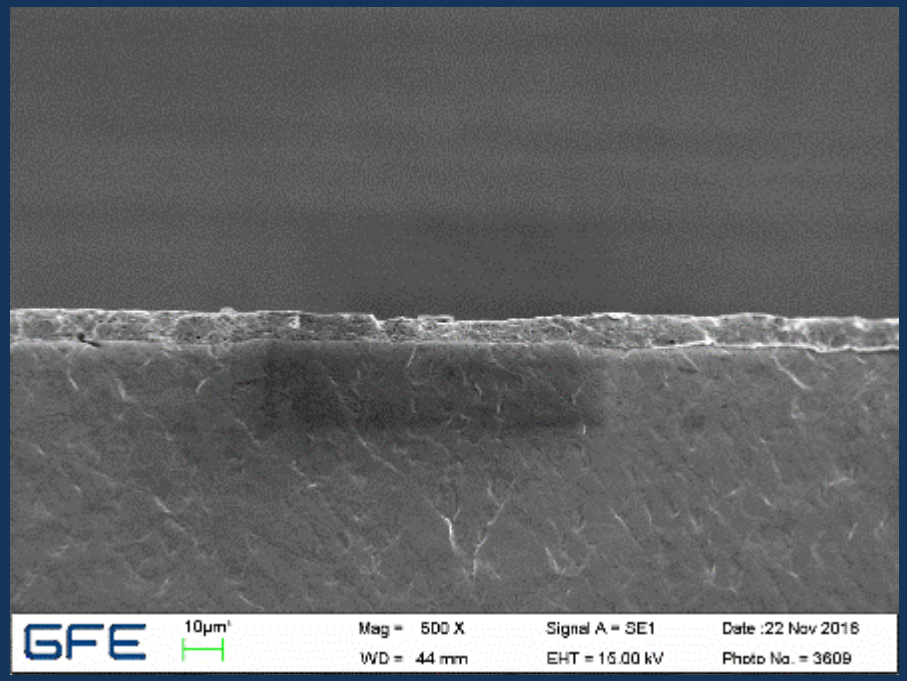

12 mm

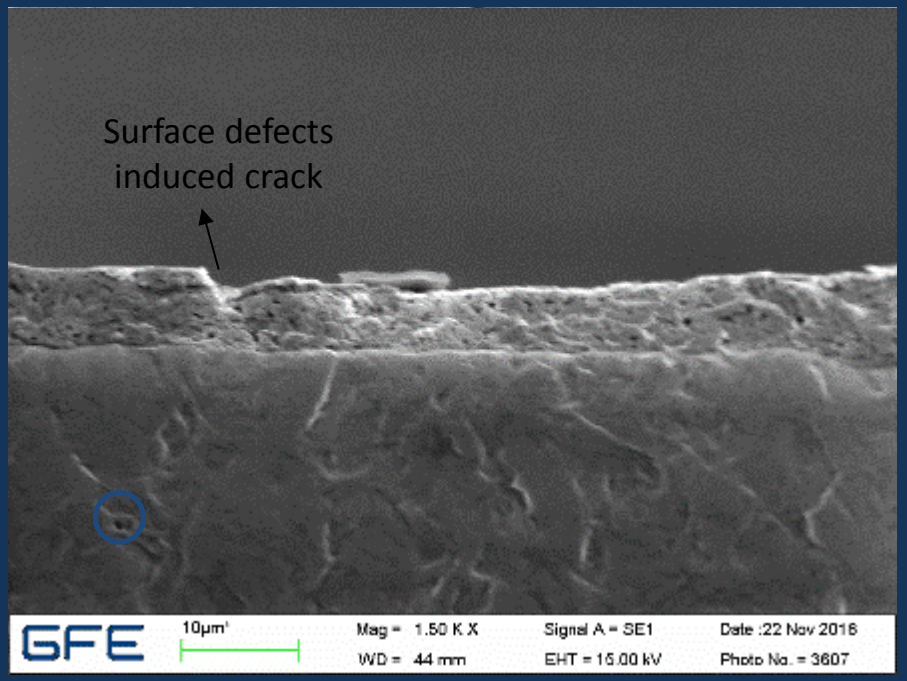

12 mm

EG DP980

Modified In-situ bending test in LC-SEM

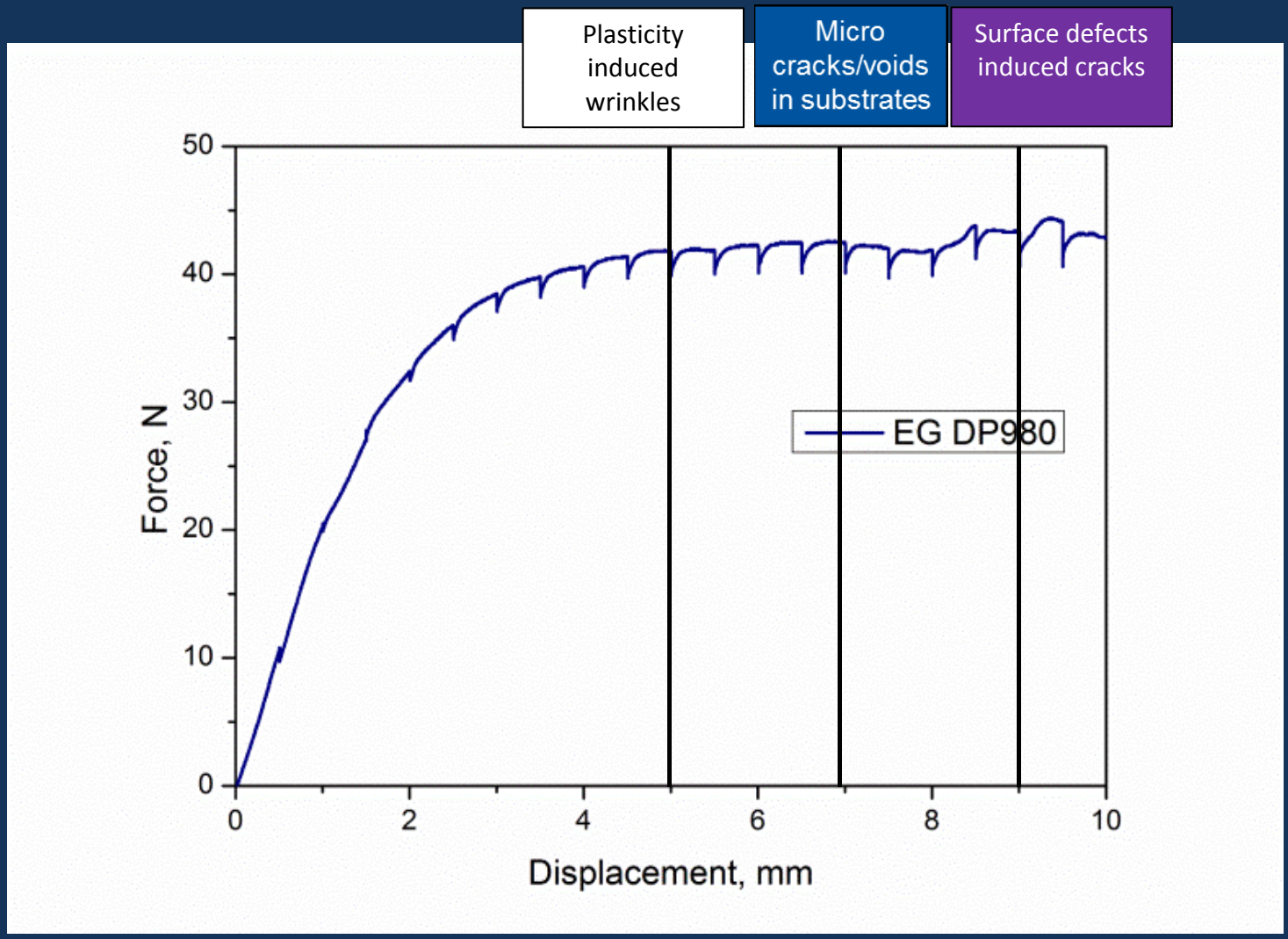

Additional work for completion of Final Report

- Micromechanical simulation analysis in Chapter 4 (now includes crystal plasticity modelling, for each of the Zn and Zn-Fe phases)
- Quantitative analysis of the crack initiation strain by digital image correlation technique in the in situ bending test in Chapter 5

III

Conclusions

- Based on the regular in situ bending test, surface micro crack occurs earlier on GA DP980 than EG DP980 and the number of surface micro-cracks on GA DP980 is much larger than that on EG DP980.
- The main crack of GA DP980 is considered to result from the large number of surface micro-cracks, while the main crack of EG DP980 is less dependent on the surface micro-cracks.
- Based on the modified in situ bending test, the surface micro cracks on the GA DP980 are revealed to be initiated mainly from the interface and partially from the intermetallic compounds. Then the crack propagates to the surface.
- The initiation of these micro cracks in the coating layers of GA DP980 is at very early deformation stage. While the initiation of the micro cracks/voids in the substrate is much later at the middle deformation stage.
- The delamination of the coating layer from the substrate occurs at the end of the deformation stage and shear induced cracks appear on the surface of the substrate.